reactions

MDPI

Review

Catalytic Oxidation Reactions for Environmental Applications: Review Article

Sabrina Antonela Leonardi, María Laura Godoy, Eduardo Ernesto Miró and Viviana Guadalupe Milt *

Instituto de Investigaciones en Catálisis y Petroquímica, INCAPE (UNL-CONICET), Facultad de Ingeniería Química, Santiago del Estero 2829, Santa Fe 3000, Argentina; sleonardi@fiq.unl.edu.ar (S.A.L.); mgodoy@fiq.unl.edu.ar (M.L.G.); emiro@fiq.unl.edu.ar (E.E.M.)

* Correspondence: vmilt@fiq.unl.edu.ar

Abstract

Catalytic oxidation is one of the most effective technologies for controlling atmospheric pollutants like carbon monoxide (CO), volatile organic compounds (VOCs), and diesel soot. Catalyst performance is governed by the interplay between reaction mechanisms, physicochemical properties, and catalyst architecture. This review provides a comprehensive overview of the fundamental oxidation pathways, including Langmuir–Hinshelwood, Eley–Rideal, and Mars–van Krevelen mechanisms, highlighting their relationship with oxygen mobility, oxygen vacancies, redox behavior, and metal–support interactions. The catalytic roles of noble metals and transition metal oxides are comparatively discussed, with emphasis on the contribution of lattice oxygen and defect chemistry to oxidation activity. The review also examines recent advances in structured catalysts designed to improve heat and mass transfer, catalyst accessibility, and practical reactor performance. Particular attention is given to biomorphic fibers, electrospun nanofibers, catalytic ceramic papers, conventional monoliths, and additively manufactured (3D-printed) monolithic structures as emerging platforms for environmental catalysis. Unlike previous reviews focused primarily on catalyst composition or individual oxidation reactions, this review integrates oxidation mechanisms, catalyst chemistry, and emerging structured catalyst architectures to provide a unified perspective on the design of efficient, durable, and scalable catalytic systems for environmental oxidation applications, while identifying key challenges and future research directions.

Keywords: catalytic oxidation; environmental catalysis; VOC oxidation; soot combustion; oxygen vacancies; mixed oxides; structured catalysts

Academic Editor: Ioannis V. Yentekakis

Received: 1 June 2026
Revised: 1 July 2026
Accepted: 10 July 2026
Published: 15 July 2026

1. Introduction

1.1. Atmospheric Contaminant Oxidation

Atmospheric pollution remains a major global concern due to its detrimental effects on human health, ecosystems, and climate. Among the most relevant air pollutants, carbon monoxide (CO), volatile organic compounds (VOCs), and particulate matter (PM, particularly soot) are of primary importance, as they are emitted from a wide range of anthropogenic sources including transportation, industrial processes, and incomplete combustion systems [1–7]. CO is a highly toxic gas that interferes with oxygen transport in the bloodstream, while VOCs contribute to the formation of photochemical smog and may exhibit carcinogenic or mutagenic properties. Soot particles, predominantly emitted from

diesel engines, are associated with severe respiratory and cardiovascular diseases and play a role in climate forcing.

To mitigate these emissions, several abatement technologies have been developed, including thermal oxidation, adsorption, and biological treatments. However, catalytic oxidation has emerged as one of the most efficient and versatile strategies for the elimination of harmful pollutants since it allows reaching high conversion levels at relatively low temperatures, thus reducing energy consumption and operational costs.

Despite the apparent simplicity, these reactions involve complex surface phenomena, including adsorption–desorption equilibria, activation of molecular oxygen, and surface redox cycles. Several mechanistic pathways have been proposed, among which the Langmuir–Hinshelwood and Eley–Rideal mechanisms are commonly invoked for CO and VOCs oxidation [8–10]. In many oxide-based catalysts, the Mars–van Krevelen mechanism plays a central role, where lattice oxygen participates directly in the oxidation process and is subsequently replenished by gas-phase oxygen. Therefore, the mobility of lattice oxygen and the formation of oxygen vacancies are key parameters governing catalytic performance. In this vein, soot oxidation is described by solid–gas–solid interactions and comprises two types of contact modes: direct and indirect. In the former (tight contact), soot particles physically interact with the catalyst whereas in the latter (loose contact), oxygen activates on the catalyst surface and diffuses to soot particles.

The catalytic oxidation of CO has been extensively studied as a model reaction in heterogeneous catalysis, providing fundamental insights into reaction mechanisms and structure–activity relationships. Noble metals such as Pt, Pd, and Au exhibit excellent activity for CO oxidation at low temperatures, although their high cost and susceptibility to poisoning have motivated the development of alternative materials [11]. Transition metal oxides, particularly those based on Co_3O_4, MnO_x, and Cu-based mixed oxides, have attracted considerable attention due to their redox properties, oxygen mobility, and relatively low cost [12].

Similarly, the catalytic oxidation of VOCs has been widely investigated due to its environmental relevance and industrial applicability [13]. VOCs encompass a broad family of organic compounds with diverse chemical structures, leading to different reactivity patterns and adsorption behaviors. Noble metal catalysts remain among the most active systems, but increasing efforts have been devoted to the development of non-noble metal catalysts, such as manganese, cobalt [14], and cerium oxides, as well as mixed oxides and perovskite-type materials [15]. The presence of water vapor and other contaminants such as sulfur compounds can significantly affect catalyst stability and performance, representing a major challenge for real-world applications.

In contrast, soot oxidation presents additional challenges due to the nature of the reaction, which involves contact between solid carbon particles and the catalyst surface. The efficiency of the process strongly depends on the quality of the contact between the solid reactant and the catalyst (loose versus tight contact conditions), as well as on the ability of the catalyst to activate oxygen and/or generate more reactive oxidizing species such as NO_2. Ceria-based materials and transition metal oxides (e.g., CoO_x [16], MnO_x [17]), have demonstrated promising performance due to their high oxygen storage capacity and redox flexibility.

From a materials perspective, catalytic systems for environmental oxidation can be broadly classified into noble metal catalysts and transition metal oxides. While noble metals offer superior intrinsic activity, transition metal oxides provide a cost-effective alternative with tunable redox properties. In addition, the use of supported and structured catalysts has gained increasing attention due to their improved heat and mass transfer characteristics and their suitability for industrial implementation.

Recent research trends are focused on the development of highly efficient, low-cost, and durable catalysts through strategies such as nanostructuring, defect engineering, and the design of multi-component systems with synergistic effects. In particular, mixed oxides based on cerium and cobalt or manganese have shown enhanced performance in the simultaneous oxidation of multiple pollutants, highlighting their potential for multifunctional environmental applications.

In this context, the present review provides a comprehensive overview of catalytic oxidation processes for the abatement of CO, VOCs, and soot, with particular emphasis on reaction mechanisms, catalyst design, and recent advances in structured catalysts. Unlike previous reviews that mainly focus on catalyst composition or individual oxidation reactions, this work emphasizes the influence of catalyst architecture—including biomorphic fibers, electrospun fibers, monolithic catalysts, and catalytic ceramic papers—on catalytic performance and practical implementation. The literature discussed in this review includes both landmark and recent peer-reviewed studies, selected according to their relevance to catalyst composition, synthesis strategy, structural configuration, physicochemical properties, and catalytic performance. By integrating advances in catalyst materials with structured catalytic systems, this review provides a broader perspective on the design of efficient and scalable catalysts for environmental oxidation applications and identifies current challenges and future research opportunities.

1.2. Bibliometric Trends in Catalytic Oxidation for Environmental Applications

To provide a quantitative overview of the evolution of research in environmental catalytic oxidation, a bibliometric analysis was performed. Searches were conducted using the terms "structured catalysts for oxidation", "CO oxidation", "VOC oxidation", and "soot oxidation". The annual scientific production and the geographical distribution of publications were analyzed in order to identify the main research trends in the areas covered by this review.

As shown in Figure 1, all four topics have experienced sustained growth during the last decade, confirming the increasing relevance of catalytic oxidation as a key strategy for pollution abatement. Among them, CO oxidation presents by far the largest scientific output, reflecting its widespread use as a model reaction for investigating catalytic activity, reaction mechanisms, oxygen mobility, and metal–support interactions. Because of its relatively simple reaction network and well-established kinetic behavior, CO oxidation has become a benchmark for evaluating novel catalytic materials before extending their application to more complex oxidation processes.

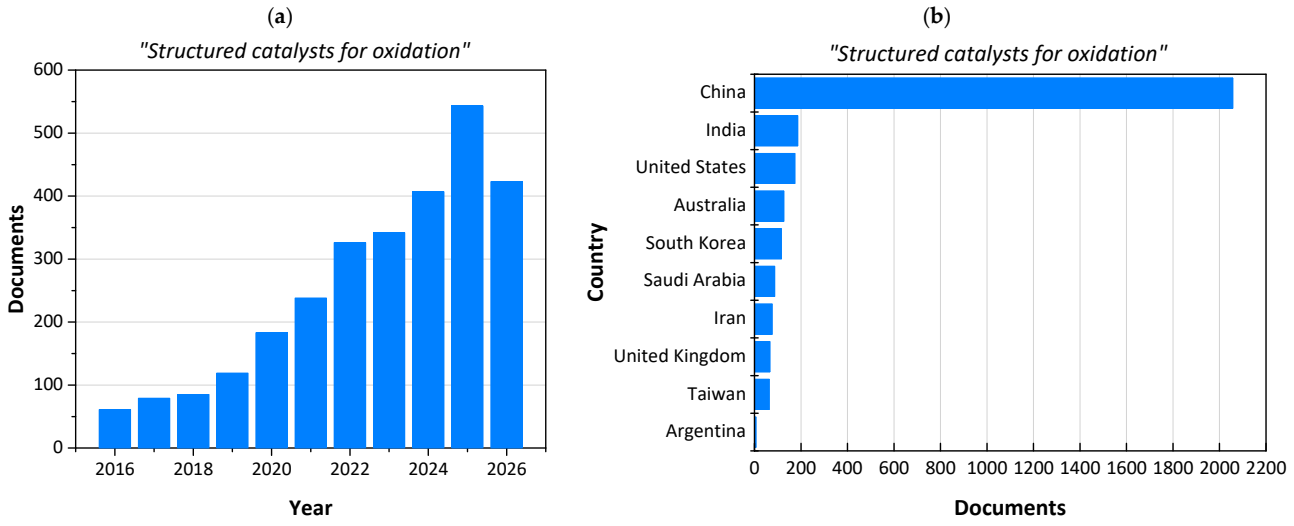

Figure 1. *Cont.*

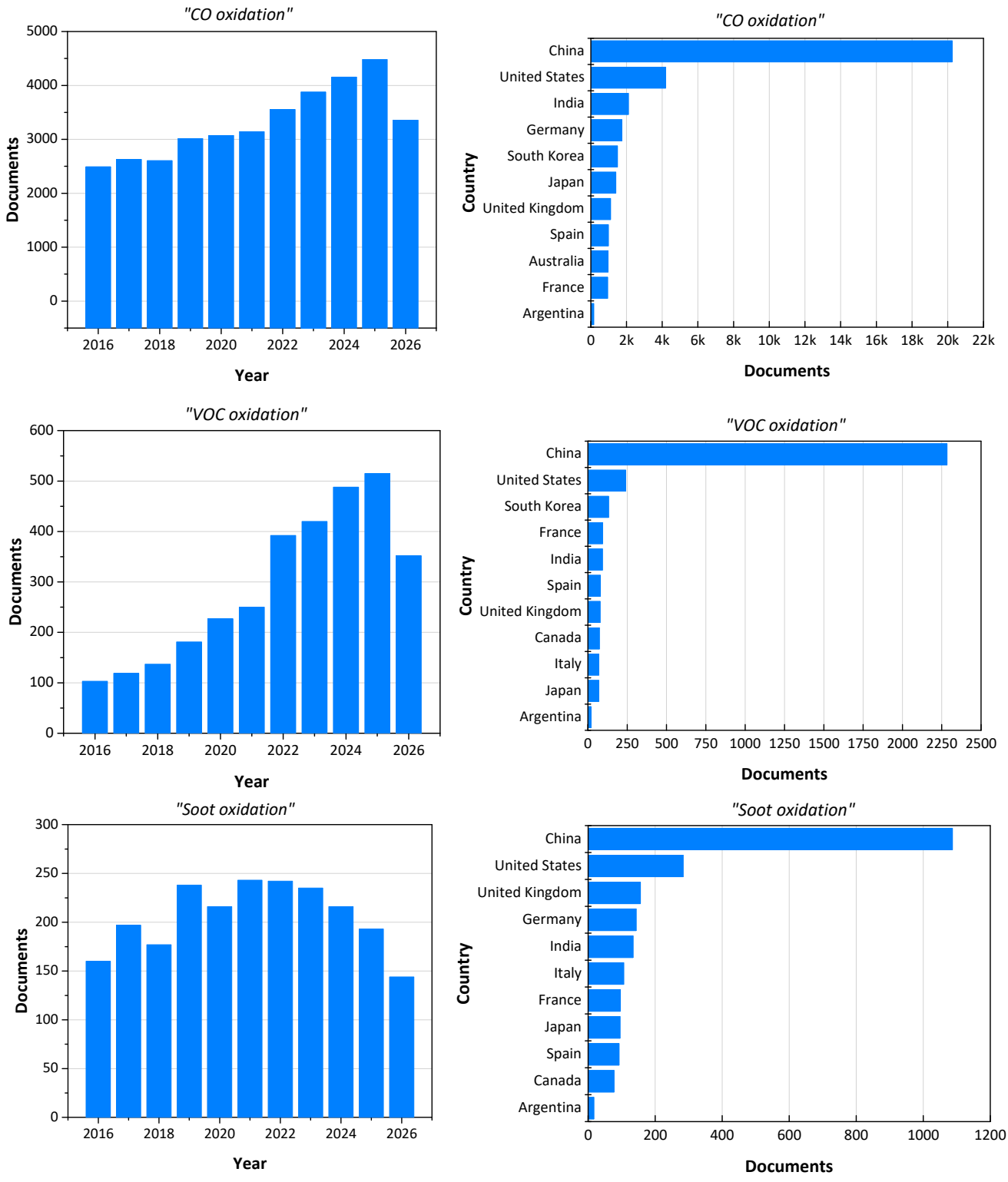

Figure 1. Bibliometric analysis of research on catalytic oxidation for environmental applications based on the Scopus database. (**a**) Annual number of publications for the topics "structured catalysts for oxidation", "CO oxidation", "VOC oxidation", and "soot oxidation". (**b**) Top contributing countries for each research area.

In contrast, research on VOC oxidation and soot oxidation has shown a steady increase driven mainly by increasingly stringent environmental regulations concerning industrial emissions and vehicle exhaust gases. Although these topics exhibit a lower publication volume than CO oxidation, their continuous growth highlights the need for catalysts

capable of operating efficiently under realistic conditions, including low temperatures, variable gas compositions, and limited catalyst–pollutant contact.

A similar upward trend is observed for structured catalysts for oxidation, indicating that current research is progressively moving beyond the optimization of catalyst composition alone. Recent studies increasingly focus on catalyst architectures that improve heat and mass transfer, reduce pressure drop, and enhance catalyst accessibility, including monolithic substrates, ceramic papers, electrospun nanofibers, biomorphic structures, and more recently, additive-manufactured catalytic systems. This evolution reflects the growing interest in translating advances achieved at the material level into structured reactors suitable for industrial implementation.

The geographical distribution of publications reveals that China is the dominant contributor across all research topics, followed by the United States and several European and Asian countries. This leadership is particularly evident for CO oxidation, where publication output is considerably higher than in the remaining areas, illustrating the strategic role of this reaction in catalyst development. At the same time, the presence of countries such as India, South Korea, Germany, the United Kingdom, France, Japan, Italy, Canada, Australia, and Argentina demonstrates that catalytic oxidation research has become a highly international field supported by active scientific communities worldwide.

Particularly in Argentina, research groups have made sustained contributions to environmental catalysis through the development of transition metal oxide catalysts, structured catalytic systems, and catalytic technologies for emission control. Recent advances include studies on electrospun oxide nanofibers, ceramic paper catalysts, stacked wire mesh monoliths and three-dimensional printed monolithic structures for CO and soot oxidation, illustrating the country's active participation in the development of innovative structured catalytic materials for environmental applications. These contributions exemplify how advances in catalyst composition and reactor architecture are being integrated to address practical challenges in pollution abatement.

The bibliometric trends indicate that current research is evolving toward the simultaneous optimization of catalyst chemistry and structured catalyst design. The increasing convergence between advanced redox materials and engineered catalytic architectures provides the scientific framework for the present review, which discusses the relationships between oxidation mechanisms, catalyst composition, oxygen transport properties, and structured catalytic systems for environmental applications.

2. Target Contaminants

2.1. Carbon Monoxide (CO)

CO is a colorless and odorless gas that is harmful when inhaled, being a main contributor to air pollution as a primary pollutant. The main outdoor sources of CO are anthropogenic such as transportation (vehicles, mainly those using gasoline) or industrial facilities (stationary), along with natural sources as well [18]. Gas heaters, chimneys, furnaces, and stoves also release CO in indoor spaces.

CO is produced as the result of an incomplete oxidation of organic compounds which occurs when there is a shortage of oxygen, and the fuel cannot react completely to produce carbon dioxide and water [19,20]. CO is easily removed from exhaust gases because it is easily adsorbed and oxidized by mobile oxygen species on the catalyst surface [21].

When breathing air with high concentration of CO, a lower amount of oxygen is transported in the blood stream due to the high affinity of hemoglobin towards CO, forming carboxy-hemoglobin (COHb) (Figure 2a). This reduces the amount of hemoglobin available to transport oxygen from the lungs to the rest of the body, thus leading to possible dizziness,

confusion, and even death. It is known as the "silent killer" since it has no clear warning of its risk [22,23].

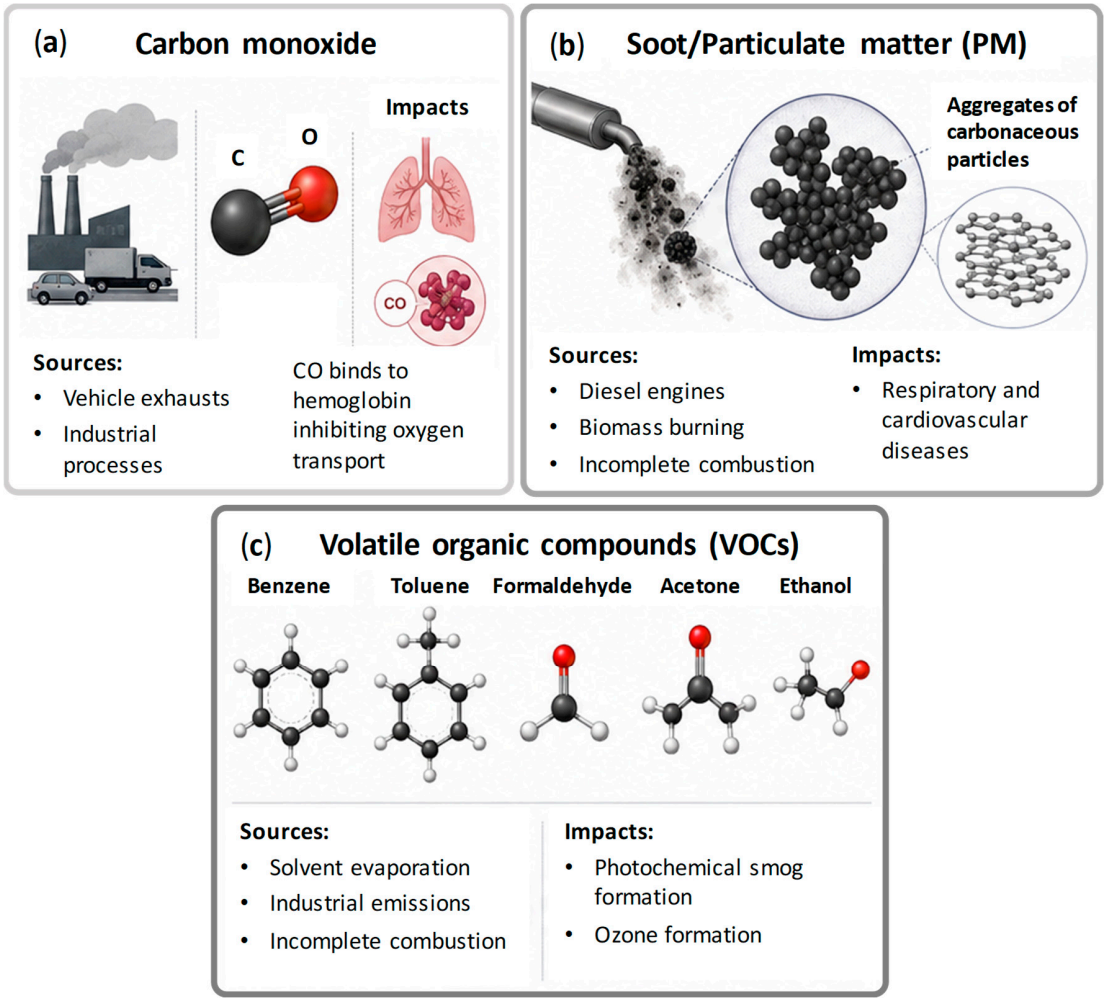

Figure 2. Main atmospheric pollutants relevant to catalytic oxidation. (**a**) Carbon monoxide, (**b**) Soot particles and (**c**) Volatile organic compounds. Ball symbols: carbon (black), hydrogen (white), oxygen (red).

2.2. Particulate Matter (PM)

PM is a main contributor to the pollution of air and is extremely dangerous upon long-term exposure. It consists of a complex mixture of solid particles and liquid droplets that vary widely in size, shape, and chemical composition (inorganic ions, metallic compounds, organic compounds and elemental carbon) depending on the source of emission. PM is commonly divided into two main categories: coarse particles (PM_{10}) and fine particles ($PM_{2.5}$), with PM_{10} and $PM_{2.5}$ referring to particles equal or lower in size than 10 μm and 2.5 μm, respectively. PM_{10} can stay suspended in air for hours or even days, and can also penetrate the lungs and remain there, whereas $PM_{2.5}$ can pass the lung barrier and even get into the blood stream. Chronic exposure to these particles can lead to serious cardiovascular and respiratory problems as well as premature death [24,25]. Particles bigger than 10 μm in size are referred to as large coarse particles and are not as dangerous as smaller ones since they usually do not enter the lungs, reaching only the nose and throat (Figure 2b).

A common source of outdoor PM are the exhaust gases from vehicles equipped with either diesel or gasoline engines, through which they exit mainly in the form of soot [26–29]. PM is also emitted from stationary engines used to generate electricity and to operate compressors, heaters and pumps at power and manufacturing plants. The composition of

PM is complex and in any particular location will be affected by local gaseous pollutants, meteorology, geography, and seasonal patterns [30].

PM released by diesel engine exhaust gases is composed of a soluble and an insoluble organic fraction. Solid carbon nuclei (soot), approximately 0.01–0.08 μm, are agglomerated with adsorbed and condensed hydrocarbons, and inorganic materials (mostly sulfates), forming bigger agglomerates of about 0.05–10 μm [29,31]. Other components found in the soluble organic fraction are aldehydes, alkanes, alkenes, aliphatic hydrocarbons, polycyclic aromatic hydrocarbons (PAHs), and even rests of lubricant oil. Inside the combustion chamber, soot is formed at elevated temperatures in fuel rich regions without sufficient oxygen, near the fuel injector. It is produced from non-burned or partially burned fuel in the vapor phase, which nucleates constituting a solid phase. The final characteristics of soot highly depend on the type and age of the engine, parameters, type of oil and fuel used [32]. All this has an effect on the number of adsorbed hydrocarbons and degree of graphitization (amorphous and graphitic contribution).

2.3. Volatile Organic Compounds (VOCs)

VOCs are a large group of carbon-based compounds that evaporate easily at ambient temperature and pressure, meaning they are present in the ambient atmosphere as vapor. Due to their high diffusivity, toxicity, and volatility, VOCs are classified as one of the major contributors to environmental pollution. Their impact in the atmosphere depends on their composition, concentration and emission source [33–35].

Most emitted VOCs can lead to the formation of secondary pollutants, such as tropospheric ozone, peroxyacetyl nitrate and secondary organic aerosols. It is well known that these pollutants cause serious environmental problems such as climate change and health effects on living beings, meaning the removal of the primary pollutants is of great importance.

VOCs come from different sources including petroleum refining and the production of organic compounds, synthetic resin and textile dyeing, as well as from printing, transportation, pharmaceutical industry, and the manufacturing of pesticides, adhesives, spraying (aerosols and air fresheners) and electronic equipment [36]. In the case of VOCs emitted from transportation, they are formed due to the incomplete combustion of the fuel in the engine, and include lineal-carbonated chain, aromatic and oxygenated compounds. Similar to PM, these sources are typically divided as “outdoor” and “indoor” [37].

VOCs include aldehydes, ketones, esters, acids and alcohols (Figure 2c). They are typically classified into different groups: halogenated (polychloromethanes, chlorobenzene, trichlorobenzene), aromatics (benzene, toluene), aliphatic hydrocarbons (saturated alkanes, unsaturated alkanes/alkenes), polycyclic aromatic hydrocarbons (naphthalene, phenanthrene, pyrene), and nitrogen- or sulfur-containing VOCs (amines, amides, nitrocompounds, methyl mercaptan, dimethyl disulfide) [33,37].

The emission of VOCs can be controlled using methods based on recovery or decomposition. The techniques based on recovery include absorption, adsorption, membrane separation, and condensation. On the other hand, decomposition methods convert VOCs into carbon dioxide and water and this oxidation process can be thermal, catalytic, or biological [34].

Thermal incineration of VOCs needs temperatures above 800 °C to achieve total oxidation and is generally applied to highly concentrated gaseous streams. In turn, the catalytic oxidation is more convenient for flue streams with low VOC concentration (<5% vol) [33]. With this approach, the oxidation can take place at much lower temperatures (250–500 °C) than using non-catalytic thermal methods.

The oxidation of VOCs containing chlorine (Cl), sulfur (S), or nitrogen (N) can lead to the formation of complex mixtures of toxic byproducts. These heteroatoms, among others,

can bring extra complications by poisoning the catalysts. In these cases, oxidation is not recommended and other processes should be used to eliminate this kind of pollutant.

2.4. Regulatory Limits and Health Outcomes

Regulatory emission limits are primarily established to protect human health and the environment; they are directly based on epidemiological and toxicological evidence linking pollutant exposure to adverse health outcomes. Numerous studies have demonstrated that both short- and long-term exposure to atmospheric pollutants, including carbon monoxide (CO), volatile organic compounds (VOCs), nitrogen oxides (NO_x), sulfur dioxide (SO_2), and particulate matter (PM), are associated with increased risks of respiratory and cardiovascular diseases, impaired lung function, neurological effects, and premature mortality. Consequently, regulatory agencies such as the World Health Organization (WHO), the U.S. Environmental Protection Agency (US EPA), and the European Union periodically update air quality guidelines and emission standards based on the latest scientific evidence regarding exposure–response relationships. It should be noted that these regulatory limits are not arbitrary threshold values but represent risk-based concentrations intended to minimize adverse health effects at the population level, although susceptible groups, including children, the elderly, and individuals with pre-existing respiratory or cardiovascular diseases, may experience health effects even at pollutant concentrations below current regulatory limits. Therefore, continuous improvement of catalytic oxidation technologies contributes not only to regulatory compliance but also to reducing the public health burden associated with air pollution.

3. Surface Reaction Mechanisms in Catalytic Oxidation Processes

3.1. Description of the Mechanisms

Catalytic oxidation reactions involved in the removal of carbon monoxide (CO), volatile organic compounds (VOCs), and diesel soot are generally described by three fundamental mechanistic frameworks: Langmuir–Hinshelwood (L–H), Eley–Rideal (E–R), and Mars–van Krevelen (MvK). These models provide the basis for understanding the interaction between reactants and catalyst surfaces, as well as the origin of active oxygen species in heterogeneous catalytic systems [9]. Figure 3 outlines the main reaction mechanisms involved in oxidation reactions for the removal of atmospheric pollutants.

The Langmuir–Hinshelwood mechanism assumes that both reactants are chemisorbed on the catalyst surface prior to reaction. In this framework, the rate-determining step typically involves the surface reaction between chemisorbed species occupying adjacent active sites. This mechanism is particularly relevant for oxidation reactions over noble metal catalysts (e.g., Pt, Pd), where both CO and O_2 can chemisorb efficiently. The reaction rate is therefore governed by the surface coverage of the adsorbed intermediates and may exhibit inhibition effects at high coverage due to site blocking [9,10].

In contrast, the Eley–Rideal mechanism involves the direct reaction between a gas-phase molecule and a chemisorbed species. In this case, only one reactant needs to be adsorbed, while the other reacts upon collision from the gas phase. This pathway becomes significant under conditions where adsorption of one of the reactants is kinetically or thermodynamically unfavorable, or at elevated temperatures where surface coverage is low. Although less commonly invoked than the L–H mechanism, it has been identified in specific oxidation systems, including CO oxidation over metal surfaces and high-temperature catalytic processes [11].

The Mars–van Krevelen mechanism represents a fundamentally different pathway, involving the participation of lattice oxygen from the catalyst. In this redox mechanism, the reactant is oxidized by oxygen species originating from the catalyst bulk, generating

oxygen vacancies that are subsequently replenished by gas-phase O_2. This mechanism is particularly relevant for reducible metal oxides, such as ceria, manganese oxides, and perovskites [10], where oxygen migration and redox properties play a crucial role in catalytic performance. The MvK mechanism is widely accepted for oxidation reactions over oxide-type catalysts, especially in the combustion of VOCs and soot oxidation, where lattice oxygen contributes significantly to activity [9–11]. In complex systems such as diesel soot oxidation, where solid–solid interactions limit adsorption equilibria, the contribution of lattice oxygen becomes particularly critical, reinforcing the relevance of the MvK mechanism in environmental catalysis.

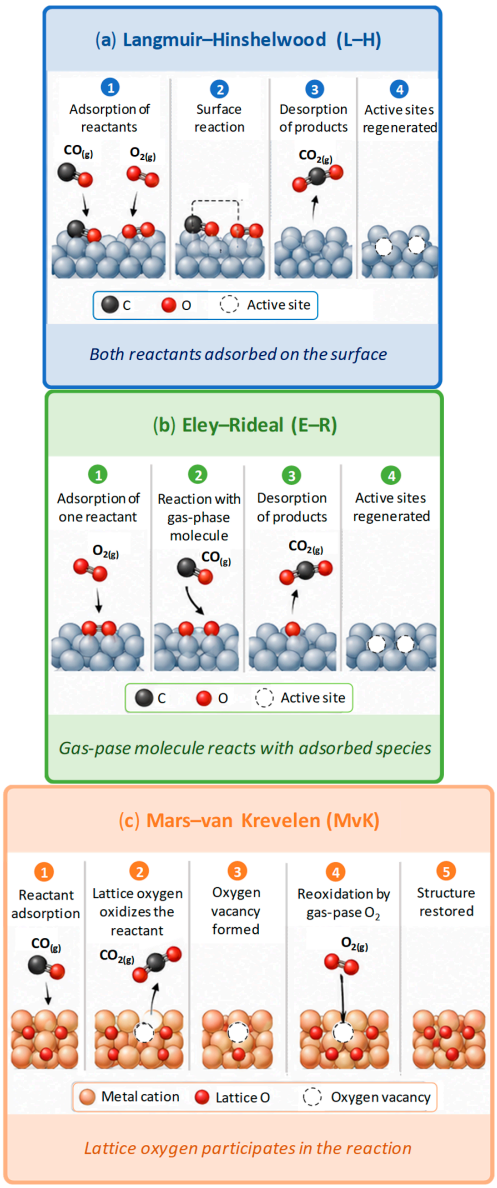

Figure 3. Representative mechanisms in catalytic oxidation reactions. (**a**) L-H, (**b**) E-R and (**c**) MvK mechanisms.

Numerous studies have demonstrated that multiple pathways may coexist, depending on catalyst composition, temperature, and reaction environment. For example, methane and VOC oxidation over supported noble metals and mixed oxides have been successfully described using hybrid kinetic models incorporating L–H, E–R, and MvK contributions [38]. In practical catalytic systems for air pollution control, the distinction between L–H, E–R,

and MvK mechanisms is often blurred, and the dominant pathway depends on catalyst reducibility, oxygen transport, and operating conditions.

3.2. Interplay Between Reaction Mechanisms and Physicochemical Properties

The prevalence of a given reaction mechanism in catalytic oxidation processes is not solely determined by reaction conditions, but is intrinsically linked to the physicochemical properties of the catalyst. In this context, parameters such as oxygen mobility, oxygen vacancy concentration, redox behavior, and metal–support interactions directly influence whether Langmuir–Hinshelwood (L–H), Eley–Rideal (E–R), or Mars–van Krevelen (MvK) pathways dominate.

In catalysts where oxygen migration and lattice oxygen availability are high, such as reducible metal oxides, the Mars–van Krevelen mechanism is typically favored. The presence of mobile lattice oxygen allows the catalyst to actively participate in the oxidation process, with oxygen vacancies acting as dynamic active sites that are continuously formed and replenished. Consequently, materials with high oxygen storage capacity and fast oxygen diffusion, such as ceria-based systems, exhibit enhanced activity in reactions where the MvK mechanism governs, including soot and VOC oxidation [39].

Conversely, in systems dominated by metallic active phases, the Langmuir–Hinshelwood mechanism becomes more relevant due to the strong adsorption of both reactants on the catalyst surface. In these cases, the catalytic performance is largely dictated by the availability and nature of surface active sites, which are strongly influenced by metal dispersion and metal–support interactions. Strong metal–support interactions can modify the electronic properties of the metal, thereby tuning adsorption energies and facilitating oxygen activation, particularly at interfacial sites [38]. This interplay often leads to synergistic effects in bifunctional catalysts, where both L–H and MvK pathways may coexist.

The Eley–Rideal mechanism, although less frequently dominant, can become significant under conditions of low surface coverage or when one of the reactants exhibits weak adsorption. In such cases, the presence of highly reactive surface oxygen species—often associated with defect sites or oxygen vacancies—can enable direct reactions with gas-phase molecules. This highlights the indirect but important role of defect chemistry in enabling alternative reaction pathways.

Overall, these observations indicate that reaction mechanisms in catalytic oxidation are not isolated phenomena but rather emerge from the dynamic interplay between surface chemistry and bulk properties. The rational design of catalysts therefore requires a simultaneous optimization of adsorption characteristics, defect density, and redox functionality to promote the most efficient reaction pathway under given operating conditions.

3.3. Experimental Discrimination Between Oxidation Mechanisms

Although the Langmuir–Hinshelwood (L–H), Eley–Rideal (E–R), and Mars–van Krevelen (MvK) mechanisms are traditionally described as distinct reaction pathways, experimental discrimination between them is often challenging because different mechanisms may coexist depending on the catalyst composition and reaction conditions. Consequently, mechanistic assignments should rely on the combination of complementary kinetic, spectroscopic, and isotopic evidence rather than on a single experimental observation [9].

Reaction kinetics provide an initial indication of the operating mechanism through the dependence of the reaction rate on reactant partial pressures, adsorption behavior, and apparent activation energies. However, kinetic analysis alone is generally insufficient to establish the reaction pathway unequivocally. Recent critical analyses have highlighted that mechanistic assignments based solely on kinetic fitting may lead to ambiguous or even misleading conclusions, particularly when multiple reaction pathways coexist [9].

Therefore, in situ and operando characterization techniques, including diffuse reflectance infrared Fourier transform spectroscopy (DRIFTS), Raman spectroscopy, X-ray photoelectron spectroscopy (XPS), X-ray absorption spectroscopy (XAS), and Temporal Analysis of Products (TAP), have become indispensable tools for elucidating oxidation mechanisms by identifying adsorbed intermediates, monitoring catalyst oxidation states, and following the evolution of surface species under reaction conditions [40,41].

Among these techniques, isotopic labeling experiments using $^{18}O_2$ are considered one of the most reliable approaches for determining the origin of the oxygen involved in oxidation reactions. The incorporation of lattice oxygen into the reaction products, followed by catalyst reoxidation by gaseous oxygen, provides strong evidence supporting a Mars–van Krevelen mechanism. Conversely, when oxygen incorporated into the products originates exclusively from adsorbed molecular oxygen, a Langmuir–Hinshelwood pathway is generally favored [40–42].

The dominant reaction mechanism depends strongly on the physicochemical properties of the catalyst and the reaction environment. As previously discussed, the Langmuir–Hinshelwood mechanism is generally favored on noble metal catalysts when both reactants are efficiently adsorbed on the catalyst surface. In contrast, the Mars–van Krevelen mechanism predominates on reducible metal oxides, mixed oxides, and perovskite catalysts possessing high oxygen mobility and abundant oxygen vacancies, where lattice oxygen actively participates in the catalytic cycle [42]. The Eley–Rideal mechanism, involving the direct reaction of a gas-phase molecule with an adsorbed species, has been proposed for several oxidation reactions but remains comparatively difficult to demonstrate experimentally. Recent assessments suggest that many reactions previously assigned to an Eley–Rideal mechanism may alternatively be explained by modified Langmuir–Hinshelwood pathways involving weakly adsorbed or highly transient surface species [9].

It is also important to recognize that these mechanisms should not always be regarded as mutually exclusive. In many practical oxidation catalysts, particularly noble metals supported on reducible oxides such as CeO_2, reaction pathways may involve simultaneous contributions from Langmuir–Hinshelwood and Mars–van Krevelen mechanisms. Under these conditions, adsorbed reactants on the metal phase react with highly mobile lattice oxygen supplied by the support through the metal–support interface, while catalyst reoxidation continuously restores the active oxygen reservoir. Consequently, the prevailing mechanism may evolve with temperature, oxygen partial pressure, catalyst reduction state, metal particle size, and metal–support interactions [9,40–42].

3.4. From Intrinsic Kinetic Models to Catalytic Reactor Design

Although intrinsic kinetic models are generally established under differential conditions to minimize transport limitations, their primary purpose is to provide reliable rate expressions for reactor design, scale-up, and process optimization. Power-law models are often used for preliminary reactor calculations, whereas mechanistic models such as Langmuir–Hinshelwood (L–H), Eley–Rideal (E–R), and Mars–van Krevelen (MvK) offer a more realistic description of surface reactions and are therefore preferred for reactor simulations involving adsorption, surface reaction, and catalyst redox cycles. These intrinsic kinetic expressions constitute the fundamental input for heterogeneous reactor models that simultaneously solve mass, momentum, and energy balances while accounting for catalyst deactivation, pressure drop, and transport limitations [43,44].

In laboratory research, catalytic oxidation kinetics are most commonly determined in differential fixed-bed tubular reactors operated under conditions that eliminate external and internal diffusion resistances, allowing intrinsic kinetic parameters to be obtained [45]. Once validated, these kinetic parameters are incorporated into reactor models to predict

the behavior of pilot- and industrial-scale systems. For VOC oxidation and other gas-phase oxidation processes, packed-bed reactors remain widely employed because of their simple design and high catalyst inventory, whereas monolithic reactors are increasingly preferred due to their low pressure drop, excellent heat-transfer characteristics, reduced diffusion limitations, and improved thermal management [43,46,47]. The interaction between intrinsic kinetics and transport phenomena becomes particularly important under highly exothermic operating conditions, where heat and mass transfer strongly influence ignition/extinction behavior, temperature gradients, and catalyst effectiveness [43,48]. Consequently, coupling mechanistic kinetic models with reactor-scale transport equations provides the essential framework for translating laboratory kinetic studies into reliable industrial reactor design and optimization.

Conventional packed-bed reactors are widely employed for the catalytic oxidation of VOCs, carbon monoxide, and other gaseous pollutants, particularly in chemical and petrochemical industries, where Langmuir–Hinshelwood and Mars–van Krevelen kinetic models are commonly incorporated into reactor simulations. Monolithic honeycomb reactors, extensively used in automotive catalytic converters and industrial air pollution control systems, combine high geometric surface area with low pressure drop, making them especially suitable for highly exothermic oxidation reactions. In regenerative catalytic oxidizers (RCOs), which are increasingly applied for the treatment of dilute VOC streams from coating, printing, pharmaceutical, and chemical industries, intrinsic kinetic models are coupled with heat and mass transfer equations to predict ignition behavior, temperature distribution, catalyst utilization, and long-term reactor performance. Therefore, mechanistic kinetic models not only provide insight into catalytic reaction pathways but also constitute the foundation for the design, scale-up, and optimization of commercial catalytic oxidation reactors [43,46,47,49].

4. Catalysts for Environmental Oxidation

4.1. Noble Metal Catalysts for Oxidation Reactions

Noble metals, particularly platinum (Pt), palladium (Pd), and gold (Au), represent one of the most effective classes of catalysts for oxidation reactions involving CO, VOCs, and diesel soot. Their high intrinsic activity is primarily associated with their ability to adsorb and activate reactants, enabling efficient oxidation at relatively low temperatures. In fact, noble metal catalysts are widely recognized for their high catalytic activity and stability, which explains their extensive use in environmental catalysis applications. However, their performance is strongly modulated by metal dispersion, particle size and interactions with the support, which can introduce additional redox functionality and enable hybrid reaction pathways [50,51]. Figure 4 shows TEM images and the particle size distribution of supported noble metals, which are widely used in oxidation reactions.

Platinum-based catalysts are widely recognized for their high activity in CO and VOC oxidation, particularly at low temperatures. This performance is largely attributed to the strong adsorption of both CO and O_2 on Pt surfaces, favoring Langmuir–Hinshelwood-type mechanisms. Additionally, Pt exhibits excellent capability for O_2 dissociation, leading to the formation of reactive oxygen species on the surface.

However, Pt also presents important limitations. One of the main challenges is its susceptibility to CO poisoning at low temperatures, where strong CO adsorption can block active sites and inhibit oxygen activation [51]. Furthermore, Pt nanoparticles tend to sinter under high-temperature conditions, reducing active surface area and long-term stability. In soot oxidation, Pt alone is often insufficient due to limited contact between the catalyst and solid carbon particles, requiring the assistance of supports with high oxygen mobility (e.g., CeO_2) to promote Mars–van Krevelen contributions.

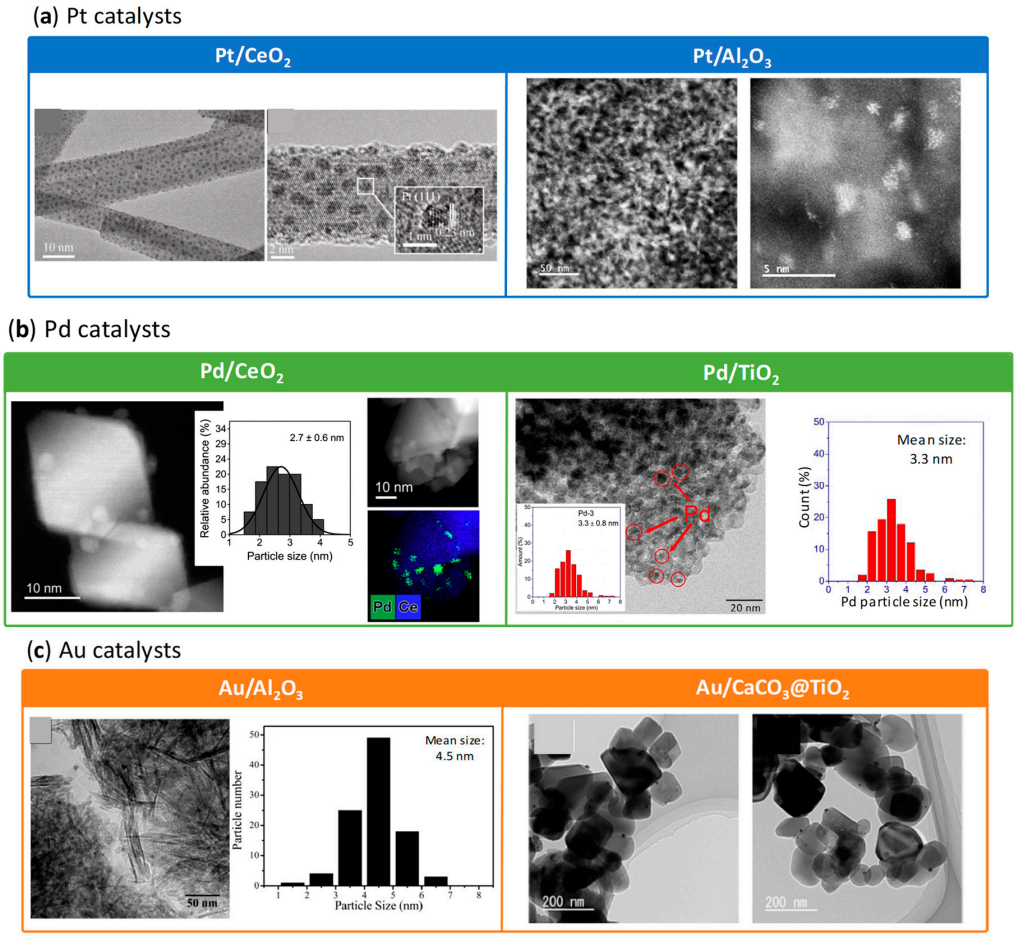

Figure 4. Representative TEM images of noble metal catalysts for catalytic reactions, which highlights the nanoscale size of Pt, Pd, or Au metal particles found in effective oxidation catalysts. (**a**), Pt/CeO_2, Adapted from [52], Figure 6a,b, https://doi.org/10.1007/s12274-010-0042-4, licensed under CC BY-NC 2.0 (https://creativecommons.org/licenses/by-nc/2.0, accessed on 30 June 2026). (**a**), Pt/Al_2O_3, Adapted from [53], Figure 7a,b, https://doi.org/10.1016/j.ijhydene.2025.152604, licensed under CC BY-NC-ND (http://creativecommons.org/licenses/by-nc-nd/4.0/, accessed on 30 June 2026). (**b**), Pd/CeO_2, Adapted from [54], Figure 6, https://doi.org/10.1002/anie.202200434, licensed under CC BY 4.0 (https://creativecommons.org/licenses/by/4.0/, accessed on30 June 2026). (**b**), Pd/TiO_2, Adapted from [55], Figure 1b, https://doi.org/10.3390/catal13111435, licensed under CC BY 4.0 (https://creativecommons.org/licenses/by/4.0/, accessed on 30 June 2026). (**c**), Au/Al_2O_3, Adapted from [56], Figure 2b, https://doi.org/10.1039/d5ra00527b, licensed under CC BY-NC 3.0 (https://creativecommons.org/licenses/by-nc/3.0, accessed on 30 June 2026). (**c**), $Au/CaCO_3@TiO_2$, Adapted from [57], Figure 4c,d, https://doi.org/10.1016/j.tsf.2025.140706, licensed under CC BY 4.0 (https://creativecommons.org/licenses/by/4.0, accessed on 30 June 2026).

Palladium is particularly effective in the oxidation of hydrocarbons and VOCs, often outperforming Pt in reactions involving more complex molecules. Pd-based catalysts exhibit a strong dependence on their oxidation state, with PdO generally considered the active phase for oxidation reactions. This introduces a significant redox component, allowing Pd systems to operate through a combination of Langmuir–Hinshelwood and Mars–van Krevelen-type mechanisms. The key advantages of Pd catalysts are their resistance to poisoning, their relatively high activity, and their adaptability in VOC oxidation systems, where they can achieve complete conversion at relatively low temperatures [50]. However, PdO is thermally unstable and can decompose into metallic Pd at high temperatures, causing fluctuations in catalytic activity. In soot oxidation, the different valance states of palladium (Pd^0, Pd^{2+}, and Pd^{4+}) play a key role. For example, in Pd/SnO_2 catalysts, the

coexistence of these species facilitates a redox cycle that promotes the Mars–van Krevelen mechanism [58]. Nevertheless, Pd-based catalysts are sensitive to water vapor, which can inhibit their performance under real exhaust conditions.

Gold catalysts have attracted considerable attention due to their remarkable activity in low-temperature CO oxidation when dispersed as nanoscale particles on oxide supports. Unlike Pt and Pd, bulk Au exhibits weak adsorption of reactants; however, Au nanoparticles can activate oxygen at the metal–support interface, emphasizing the importance of strong interactions. This often leads to synergistic effects between the metal and the support, enabling reaction pathways that combine adsorption and redox processes. Recent reviews highlight that catalytic performance in Au systems is highly dependent on particle size, support properties, and interfacial structure [51,59], with Au nanoparticles generally exhibiting enhanced CO oxidation activity as particle size decreases to the nanoscale. Nevertheless, the particle size–activity relationship is not universal and may strongly depend on the support and preparation method. For example, Petkov et al. [60] reported that Au nanoparticles prepared through a preformed nanoparticle route and deposited on TiO_2 and SiO_2 exhibited contrasting trends: catalytic activity decreased with decreasing particle size on TiO_2, whereas the opposite behavior was observed on SiO_2. The authors attributed these differences to support-dependent structural modifications of the Au nanoparticles, variations in the population of low-coordinated surface atoms, and distinct metal–support interactions induced during catalyst preparation and thermal treatment. Guo et al. [61] supported uniform 2 nm Au nanoparticles on iron oxides that exhibited high catalytic activity, attributed to effective interactions between the gold and the support. Milt et al. [62] studied both a powder Au/TiO_2 catalyst where Au nanoparticles had 3–4 nm diameter and a structured catalyst supporting this powder catalyst on AluchromYHf monoliths, where Au nanoparticles increased their average diameter to 9 nm. The catalytic activity of the powder and structured catalysts was tested in the oxidation of the CO reaction, where both the powder and the structured catalysts demonstrated to be active at room temperature. Moreover, in spite of their larger gold particle size, the catalytic activities of the structured catalysts overcame those of the powder catalyst, probably due to the segregation of the transition metal oxides from the metallic substrate toward the surface catalytic coating.

On the other hand, Della Pina et al. [63] found that small and well-dispersed Au nanoparticles supported on reducible oxides exhibit remarkable activity for the total oxidation of VOCs at relatively low temperatures.

Recently, single-atom catalysts (SACs) have emerged as a promising alternative to conventional noble metal nanoparticles for environmental oxidation reactions [64]. In these systems, isolated metal atoms are stabilized on suitable supports, maximizing metal utilization efficiency while creating well-defined active sites. SACs based on Pt, Pd, Au, and other non-noble metals have demonstrated remarkable activity for CO and VOC oxidation [65], often exhibiting distinct reaction pathways and enhanced resistance to sintering compared with nanoparticle-based catalysts [66]. Furthermore, the strong interaction between isolated metal atoms and reducible oxide supports can promote oxygen activation and facilitate redox processes. In addition to their excellent catalytic performance, SACs constitute valuable model systems for understanding reaction mechanisms and guiding the rational design of highly efficient oxidation catalysts. Although the development of SACs is still predominantly focused on powder catalysts, their incorporation into structured catalytic architectures represents an attractive strategy for future environmental applications.

As a summary, noble metal catalysts exhibit high activity in oxidation reactions primarily due to their strong adsorption properties and ability to activate oxygen. However, their performance is not solely determined by the metal itself, but by its interaction with the support and its ability to access additional redox functionalities. While Pt and Pd are

typically associated with Langmuir–Hinshelwood pathways, the incorporation of reducible supports enables the participation of Mars–van Krevelen-type mechanisms, particularly in reactions where oxygen mobility and vacancy formation are critical, such as soot oxidation. Gold catalysts, in contrast, highlight the importance of interfacial effects, where catalytic activity emerges from the synergy between metal nanoparticles and oxide supports [51].

4.2. Transition Metal Oxide Catalysts for Oxidation Reactions

Transition metal oxides have emerged as highly promising alternatives to noble metals for catalytic oxidation processes due to their lower cost, high thermal stability, and intrinsic redox properties. Among them, Co_3O_4, MnO_x, and CeO_2 are extensively studied for the oxidation of CO, VOCs, and diesel soot. In contrast to noble metals, their catalytic performance is primarily governed by lattice oxygen participation, oxygen vacancy formation, and redox cycling, making them particularly suitable for Mars–van Krevelen-type mechanisms.

Co_3O_4 is widely recognized as one of the most active transition metal oxides for low-temperature oxidation reactions. Its superior catalytic performance is mainly attributed to the coexistence of Co^{2+}/Co^{3+} redox couples and the presence of highly reactive surface oxygen species. These features facilitate rapid oxygen exchange and promote oxidation via Mars–van Krevelen pathways.

Recent studies highlight that Co_3O_4-based catalysts exhibit excellent activity in VOC oxidation due to their high oxygen migration and facile redox cycling [67], enabling efficient activation of oxygen species at relatively low temperatures. Moreover, the catalytic performance of Co_3O_4 is highly sensitive to morphology, exposed crystal planes, and defect density, which directly influence oxygen vacancy concentration and reactivity.

Co_3O_4 also presents limitations, including moderate resistance to water and sulfur poisoning, as well as lower intrinsic activity compared to noble metals under certain conditions. These drawbacks have driven the development of mixed oxides (e.g., with MnO_2 or CeO_2) and supported systems to improve stability and activity.

On the other hand, MnO_x catalysts are particularly attractive due to their multiple accessible oxidation states (Mn^{2+}, Mn^{3+}, Mn^{4+}), which provide exceptional redox flexibility. This property enables efficient participation in oxidation reactions through dynamic redox cycles and enhances the formation of reactive oxygen species. In addition to the strong dependence of catalyst activity with Mn oxidation state distribution, the structural form influences both oxygen mobility and vacancy formation. Recent studies show that MnO_x-based catalysts exhibit high activity in the oxidation of CO and VOCs, especially when supported on other oxides to enhance oxygen activation capacity [68]. Furthermore, MnO_x has shown significant potential in promoting oxidation reactions when coupled with Co_3O_4 or CeO_2, where synergistic interactions improve reducibility and oxygen transfer, thereby lowering activation temperatures and enhancing catalytic efficiency.

Additionally, CeO_2 is one of the most extensively studied oxides in environmental catalysis due to its unique redox properties and oxygen storage capacity. The reversible Ce^{4+}/Ce^{3+} redox cycle enables the formation and healing of oxygen vacancies, which are essential for oxygen activation and transport.

Recent reviews emphasize that CeO_2 exhibits high oxygen vacancy concentration and remarkable oxygen migration [69], making it particularly effective in oxidation reactions governed by Mars–van Krevelen mechanisms. These properties allow CeO_2 to act not only as an active catalyst but also as an oxygen buffer, continuously supplying reactive oxygen species during the catalytic cycle. In soot oxidation, CeO_2 plays a crucial role by facilitating oxygen transfer to the carbon surface, overcoming limitations associated with poor catalyst–soot contact. However, pure CeO_2 often exhibits lower intrinsic activity compared to Co_3O_4 or noble metals.

Overall, transition metal oxides differ fundamentally from noble metals in that their catalytic activity is primarily governed by bulk and lattice properties rather than surface adsorption alone. High oxygen mobility, abundant oxygen vacancies, and strong redox capabilities promote Mars–van Krevelen-type mechanisms, making these materials particularly effective for oxidation processes involving complex molecules and solid substrates such as soot. The design of efficient catalysts therefore relies in optimizing these properties, often through the development of mixed oxide and engineered nanostructures that enhance oxygen transport and defect chemistry.

4.3. Mixed Oxides

Among mixed oxide systems, Ce–Mn catalysts have attracted significant attention due to their outstanding redox synergy and enhanced oxygen transfer properties. The combination of ceria and manganese oxides leads to a substantial increase in oxygen vacancy concentration and improved reducibility compared to the individual oxides, as widely reported in recent studies on Ce–Mn catalysts for VOC oxidation and CO abatement [70,71].

This behavior arises from the strong electronic interaction between Ce^{4+}/Ce^{3+} and Mn^{4+}/Mn^{3+} redox couples, which facilitates electron transfer and promotes the formation of highly reactive oxygen species. As a result, Ce–Mn systems exhibit enhanced oxygen migration and faster lattice oxygen exchange, making them particularly effective for Mars–van Krevelen-type oxidation pathways [72]. Additionally, structural factors such as intimate mixing, solid solution formation and defect-rich interfaces further enhance catalytic activity by increasing the density of active sites and facilitating oxygen diffusion.

From a mechanistic perspective, Mn species often act as active redox centers, while ceria provides an oxygen buffer function, stabilizing vacancies and enabling rapid reoxidation. This dual functionality significantly improves catalytic performance in CO and VOC oxidation, as well as in soot combustion, where oxygen transfer to the carbon surface is rate-limiting.

Ce–Co systems represent another important class of mixed catalysts where strong synergistic effects arise from the interaction between ceria and cobalt oxide phases. In these materials, Co_3O_4 provides highly active redox sites, while CeO_2 enhances oxygen transport and stabilizes the catalyst structure. The interaction between Co_3O_4 and CeO_2 leads to increased oxygen vacancy formation and improved reducibility, which significantly enhances catalytic activity in oxidation reactions [73]. In soot oxidation, this synergy facilitates oxygen transfer to the carbon surface, which enhances the efficiency of Mars–van Krevelen cycles, lowers ignition temperatures, and improves catalytic efficiency [74,75].

A key feature of Ce–Co systems is the formation of interfacial sites where oxygen activation is significantly enhanced. These sites can facilitate both adsorption-driven and redox-driven pathways, effectively bridging Langmuir–Hinshelwood and Mars–van Krevelen mechanisms.

Moreover, ceria plays a critical role in improving the thermal stability of cobalt oxide, mitigating sintering and maintaining catalytic activity under harsh conditions. This makes Ce–Co catalysts particularly attractive for real exhaust applications.

Perovskite oxides (general formula ABO_3) represent a highly versatile class of catalysts, where catalytic properties can be finely tuned through compositional and structural modifications. Their flexibility allows for precise control of oxygen vacancies, redox behavior, and metal–oxygen bond strength. In these systems, the A-site (typically rare earth or alkaline earth metals) influences structural stability and oxygen mobility and the B-site (transition metals such as Co, Mn, Fe) determines redox activity and catalytic functionality.

One of the most important features of perovskites is their ability to accommodate non-stoichiometry, leading to the formation of oxygen vacancies and highly mobile lattice

oxygen [76]. This makes them particularly effective for oxidation reactions governed by Mars–van Krevelen mechanisms [77].

Furthermore, partial substitution at the A- or B-site can enhance oxygen vacancy concentration, improve electronic conductivity and tune adsorption properties.

From a mechanistic standpoint, perovskites often operate via combined pathways, where lattice oxygen participates in oxidation while surface adsorption processes also contribute. This dual behavior enables high catalytic activity across a wide temperature range.

In soot oxidation, perovskites are especially promising due to their ability to facilitate oxygen transfer and maintain activity under limited contact conditions. Their structural robustness and resistance to sintering further enhance their applicability in real systems.

The enhanced performance of Ce–Mn, Ce–Co, and perovskite systems clearly demonstrates that catalytic activity in oxidation reactions is not dictated by a single property, but rather by the synergistic coupling of oxygen mobility, vacancy formation, and redox dynamics. These materials effectively bridge the gap between surface-driven and lattice-driven mechanisms, enabling optimized catalytic pathways under practical operating conditions.

These synergistic systems highlight that the most effective catalysts are not those maximizing a single property, but those optimizing the dynamic interplay between oxygen activation, transport, and surface reactivity.

Figure 5 shows examples of structures and micrographs of oxide mixtures and perovskite-type mixed oxides.

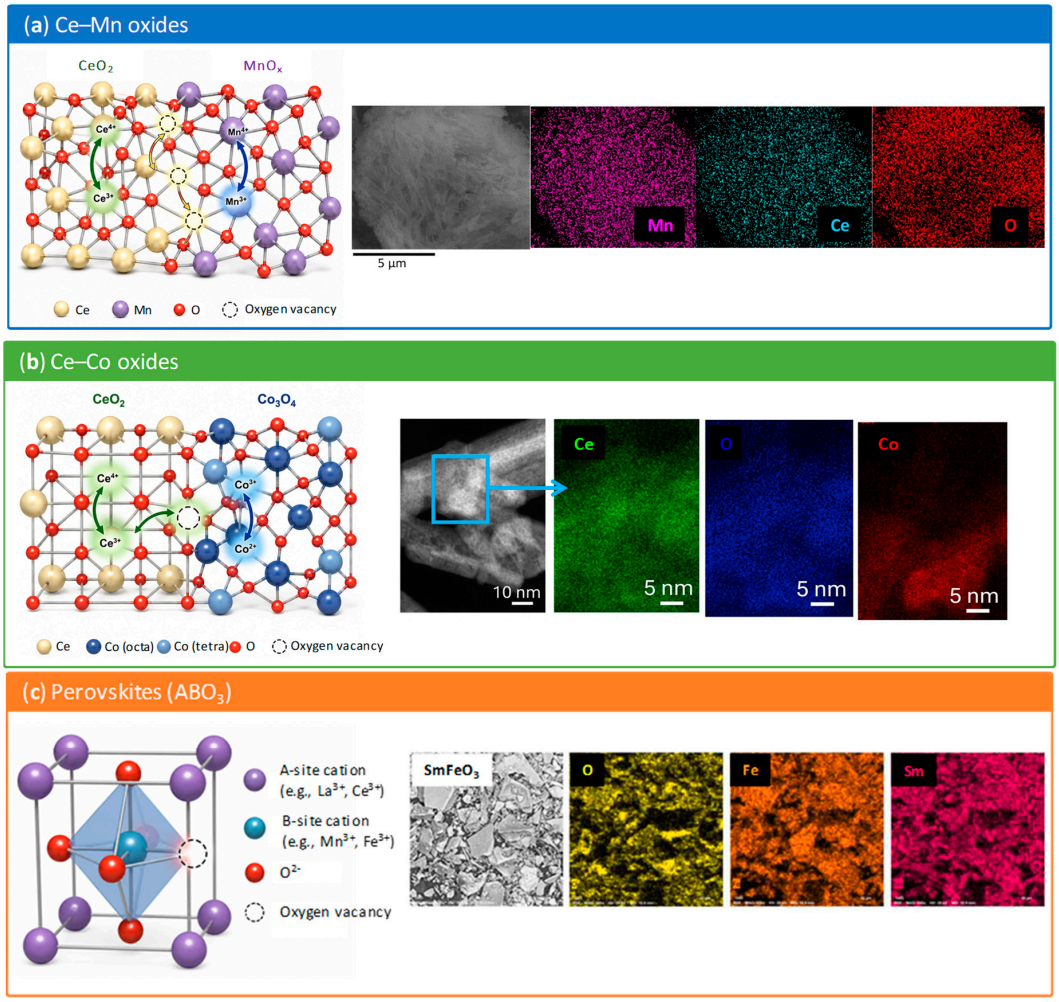

Figure 5. Mixed-oxide and perovskite catalysts: oxygen vacancies and enhanced oxygen mobility. (**a**), Adapted from [78], Figure 3h–k, https://doi.org/10.1016/j.catcom.2023.106832, licensed under

4.4. Catalyst Stability: Deactivation and Regeneration Strategies

Catalyst stability is a critical requirement for the practical implementation of oxidation catalysts, as high initial activity alone is insufficient to guarantee long-term performance under industrial operating conditions. Catalyst deactivation may arise from thermal sintering of the active phase, poisoning by sulfur-, chlorine-, or phosphorus-containing compounds, carbon deposition, phase transformations, volatilization of active species, and changes in the metal–support interaction during prolonged operation. The relative importance of each deactivation mechanism depends on the catalyst composition, support properties, reaction temperature, and gas composition. Therefore, catalyst durability should be considered together with activity and selectivity during catalyst design [81,82].

Noble metal catalysts, particularly Pt- and Pd-based materials, generally exhibit excellent catalytic activity at low temperatures and high resistance toward carbon deposition. However, their long-term stability is frequently limited by thermal and hydrothermal sintering, which leads to particle growth, loss of metal dispersion, and consequently a decrease in the number of accessible active sites. Repeated oxidation–reduction cycles may also induce structural reconstruction of the metal nanoparticles or encapsulation by the support. To minimize these effects, noble metals are commonly dispersed on thermally stable reducible oxides, such as CeO_2, or on mixed oxides capable of generating strong metal–support interactions (SMSI), which suppress metal mobility and preserve the active surface during aging. Védrine emphasizes that the combination of noble metals with oxygen-storage materials represents one of the most successful approaches to simultaneously enhance catalytic activity and durability [82].

Compared with noble metals, transition metal oxides such as MnO_x, CoO_x, CuO_x and FeO_x generally exhibit superior thermal stability, lower cost, and greater tolerance to high-temperature operation. Nevertheless, these catalysts may undergo changes in oxidation state, oxygen vacancy concentration, crystallinity, and surface area during prolonged operation. Because their catalytic performance strongly depends on lattice oxygen mobility and redox cycling, irreversible structural modifications may gradually reduce oxygen transfer rates and catalytic activity. In particular, manganese oxides are susceptible to phase transformations among MnO_2, Mn_2O_3 and Mn_3O_4 depending on the reaction atmosphere and temperature, whereas copper oxides may suffer partial reduction and sintering under reducing environments [82].

Mixed metal oxides generally exhibit higher structural stability than single oxides owing to synergistic interactions between different cations. Spinel- and perovskite-type oxides, as well as Ce–Mn, Ce–Co and Ce–Cu mixed oxides, display improved oxygen mobility, enhanced resistance to phase segregation, and greater tolerance to thermal aging. In ceria-containing mixed oxides, the Ce^{4+}/Ce^{3+} redox couple promotes reversible oxygen storage and facilitates the regeneration of oxygen vacancies, thereby preserving catalytic performance during repeated oxidation–reduction cycles. Furthermore, incorporation of a second metal often inhibits crystallite growth and stabilizes the catalyst structure at elevated temperatures. These synergistic effects explain why mixed oxides frequently outperform both noble metal-free single oxides and unsupported noble metals in long-term oxidation reactions.

Catalyst poisoning represents another important cause of deactivation in oxidation processes. Sulfur-containing compounds can form stable sulfates on both noble metals and transition metal oxides, blocking active sites and decreasing oxygen mobility. Water vapor may competitively adsorb on oxygen vacancies or hydroxylate the catalyst surface, while chlorine-containing compounds can modify surface acidity and alter the oxidation state of active species. In general, noble metal catalysts exhibit better resistance toward water inhibition, whereas mixed oxides containing ceria have demonstrated improved sulfur tolerance because of their higher oxygen storage capacity and faster regeneration of active oxygen species.

As a matter of fact, catalyst stability is governed not only by the intrinsic properties of the active phase but also by catalyst architecture. Strategies such as optimizing metal–support interactions, increasing oxygen storage capacity, designing mixed oxides with high structural robustness, and controlling particle size have become essential for developing oxidation catalysts capable of maintaining high activity during long-term operation under realistic reaction conditions [82].

Catalyst regeneration has become an increasingly important aspect in the practical application of oxidation catalysts, as it extends catalyst lifetime, reduces replacement costs, and improves process sustainability. The most common regeneration strategy is thermal oxidative treatment, which removes carbonaceous deposits and restores active oxygen species on the catalyst surface. This approach is particularly effective when catalyst deactivation is mainly caused by coke deposition or reversible changes in the oxidation state of transition metal oxides [81,82].

For catalysts deactivated by sulfur-containing compounds, regeneration is considerably more challenging because stable sulfate species may form on both the active phase and the support. In these cases, high-temperature treatments under reducing atmospheres, alternating lean/rich cycles, or sequential reduction–oxidation treatments have proven effective for decomposing sulfate species and recovering catalytic activity. The regeneration efficiency strongly depends on the catalyst composition and support. For example, Pd–Pt catalysts supported on ceria–zirconia exhibit faster sulfur removal and higher activity recovery than alumina-supported catalysts because reducible oxides facilitate sulfate decomposition and oxygen exchange [83,84].

For transition-metal oxide catalysts, regeneration generally relies on thermal treatment in air, which restores the original oxidation state and replenishes oxygen vacancies. In ceria-containing mixed oxides, the reversible Ce^{4+}/Ce^{3+} redox cycle contributes to self-regeneration by promoting oxygen mobility and facilitating the recovery of lattice oxygen during operation. Recent studies have also explored alternative regeneration methods, including steam-assisted treatments, washing procedures for sulfate removal, and non-thermal plasma, which enables coke oxidation at relatively low temperatures while minimizing thermal sintering. Although these approaches remain largely at the laboratory scale, they represent promising strategies for improving catalyst durability in industrial oxidation processes [85,86].

Catalyst regeneration should be considered during catalyst design, together with activity, selectivity, and stability. Developing catalysts that can be efficiently regenerated after sulfur poisoning, hydrothermal aging, or carbon deposition represents an important direction for the practical implementation of catalytic oxidation technologies.

5. Structured Catalysts for Oxidation Reactions

In catalytic oxidation processes for CO, VOCs, and diesel soot removal, catalyst performance is determined not only by the intrinsic activity but also by the micro- and macroscopic architecture of the catalytic system. Structured catalysts have been extensively

developed to overcome transport limitations, improve heat management, and enhance contact between the catalyst and the reactants under real operating conditions [87,88]. Examples of microscopic structures are fibers, while macroscopic structures involve monolithic substrates—whether stacked metal meshes, or those obtained via 3D printing—as well as ceramic papers. These structures represent key configurations with distinct advantages depending on the intended application.

5.1. Fibers as Microstructure Catalytic Supports for Oxidation Reactions

Among the various morphologies commonly used for catalysts design, fiber-based materials have gained much interest.

Fibers are elongated elements which typically have cylindrical geometries with a wide range of diameter sizes, from nanometers to millimeters and they can be made from different kinds of materials, including ceramic and metallic ones. In addition, isolated fibers can be used to form macrostructures when knitted or pressed. This variety of possibilities makes fibers very attractive since they can be specifically produced to fit desired applications.

Fibrous materials are promising in the field of catalysis due to the following characteristics: high length to diameter ratio (aspect ratio), high surface to volume ratio, low pressure drop, high mass transfer and void fraction, safe handling, easy scale-up, and low costs of manufacture [89,90]. Fibrous catalysts are classified as micro-structured catalysts that satisfy the important requirements of catalyst effectiveness and low pressure drop, which is not easily achieved with catalytic pellets in packed beds. The small dimensions of fibers can eliminate diffusion as a rate-controlling factor by providing short diffusion distances. The radial mixing of a fluid is improved by the tortuosity of the fibrous bed, which can also provide uniform temperature and concentration profiles. The low resistance to flow of liquids and/or gases passing through the fibers is one of the main advantages, which is related to their low pressure drop [90,91].

Concerning the materials which catalytic fibers are made of, they are generally divided into: metallic, glass, ceramic, and carbon. Metallic fibers (thin wires and metallic filaments) can be used as unordered sintered metal fiber sheets for filter application or ordered knitted or woven wire mesh structures. The most common examples of metallic substrates are wire meshes and gauzes [89,90].

Some properties of glass-fiber catalysts are high specific surface area, low cost, good flexibility, and inertness. Ceramic fibers are made from combinations of kaolin, alumina, quartz, zirconium oxide and other oxides, that add specific properties such as good thermal stability (better than metallic fibers), mechanical resistance, flexibility, and high specific surface area (if there is good porosity) [89,90]. On the other hand, carbon-based fibers present specific surface areas in the range of 1500–3000 m^2/g, high adsorption capacity, as well as a unique type of surface, being able to have a complex porous structure (microporous, mesoporous, and macroporous) [92,93].

5.1.1. Biomorphic Fibrous Catalysts

Biomorphic fibrous catalysts have emerged as a highly promising class of structured materials for oxidation reactions, particularly in diesel soot abatement, due to their unique hierarchical architecture derived from natural templates. These materials preserve the intrinsic microstructure of biomass precursors, resulting in interconnected fibrous networks whose porosity and low-pressure drop enhance mass transport, oxygen diffusion, and catalyst–soot contact efficiency. They have also been tested for CO oxidation and VOCs combustion.

The synthesis of biomorphic fibers typically involves the transformation of natural templates, such as cotton or wood, into inorganic replicas through controlled thermal and chemical treatments (Figure 6a). This approach enables the formation of micro- and nanostructured oxides, including CeO_2, Co_3O_4, MnO_x and mixed systems such as Ce–Co and Ce–Mn (Figure 6b), with high surface area and tunable redox properties.

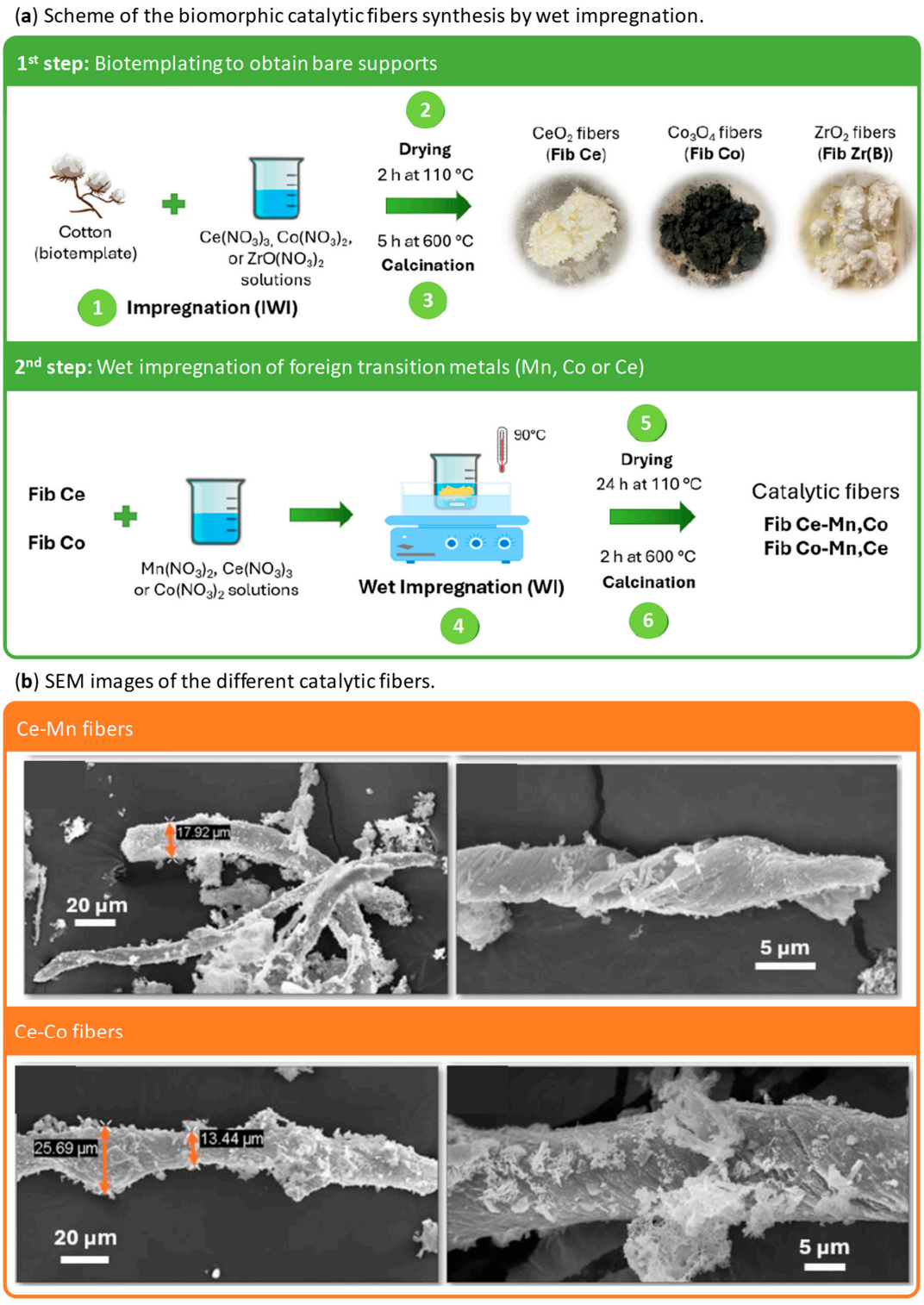

Figure 6. Biomorphic catalytic fibers reported by Rodriguez [94]. (**a**) Procedure for obtaining catalytic ceramic fibers through biomorphic synthesis. (**b**) SEM images (different magnifications) of CeO_2 catalysts deposited on either biomorphic Mn or Co fibers.

A key feature of these materials is their ability to generate abundant oxygen vacancies and promote rapid redox cycling, particularly in ceria-based systems. The incorporation of transition metals such as cobalt or manganese further enhances catalytic performance through synergistic effects, improving oxygen mobility and facilitating lattice oxygen participation in oxidation reactions. As a result, these catalysts often operate via Mars–van Krevelen-type mechanisms, which are particularly relevant in soot oxidation.

From a structural perspective, the fibrous morphology plays a decisive role in catalytic performance. The high aspect ratio and interconnected porosity promote intimate contact between soot particles and catalytic sites, overcoming diffusion and contact limitations commonly observed in conventional catalysts. Additionally, the distribution of the active phase—whether as surface-deposited nanoparticles or integrated within the fiber matrix—strongly influences catalytic activity and stability.

Biomorphic ceramic fibers have been studied either as bulk catalysts or as support of catalysts, with the aim of obtaining microstructured catalysts. Stegmayer et al. [95] studied the development of biomorphic cobalt oxide and ceria microfibers obtained from natural cotton templates and demonstrated their application in diesel soot oxidation. Their work showed that the biomorphic synthesis route enabled the preservation of the fibrous morphology after calcination, generating highly porous structures with enhanced soot–catalyst contact efficiency. In particular, cobalt-containing fibers exhibited improved reducibility and oxygen mobility, which promoted soot combustion at lower temperatures. The study highlighted the importance of combining the redox properties of transition metal oxides with the structural advantages of biomorphic supports.

Subsequent studies expanded this approach by incorporating additional active phases onto biomorphic ceria fibers. Rodriguez et al. [96] investigated the plasma-assisted deposition of Mn and Fe species on CeO_2 biomorphic fibers for soot combustion and CO oxidation. The use of gliding arc plasma allowed efficient surface functionalization and homogeneous dispersion of the active phases while preserving the fibrous architecture. The authors reported that Mn deposition significantly enhanced catalytic activity due to improved oxygen exchange capacity and the formation of surface oxygen vacancies, whereas Fe-containing systems also contributed to redox activity and catalytic stability. The study demonstrated that plasma-assisted methods represent an effective strategy for tailoring the surface chemistry of biomorphic catalysts.

In a related work, Rodriguez et al. [97] further explored Mn- and Co-decorated biomorphic ceria fibers for soot combustion and benzene total oxidation. Both transition metals improved catalytic performance compared with bare ceria fibers, although different behaviors were observed depending on the target reaction. Mn-containing catalysts exhibited enhanced activity associated with higher oxygen migration and defect concentration, while cobalt-containing samples showed strong redox properties that are favorable for oxidation reactions. Importantly, the fibrous morphology facilitated gas accessibility and promoted efficient interaction between the catalyst surface and the reacting species, particularly in soot oxidation where contact phenomena are critical.

The versatility of biomorphic fibers was further demonstrated by Sacco et al. [98], who synthesized cotton-derived Mn–Ce and Mn–Co–Ce biomorphic fibers and evaluated their catalytic performance in soot combustion and CO oxidation. Their results confirmed that the incorporation of mixed oxide compositions by means of the traditional wet impregnation method generated synergistic redox interactions that improved reducibility and surface oxygen availability. The Mn–Co–Ce systems exhibited particularly high catalytic activity due to the combined effects of ceria oxygen storage capacity and the redox cycling ability of manganese and cobalt species. Additionally, the preservation of the biomorphic fibrous structure contributed to improved reactant diffusion and thermal resistance.

Complementary insights into plasma-assisted deposition techniques were provided by Leonardi et al. [99], who studied the deposition of Fe and Mn oxides on fibrous ceramic supports using gliding arc plasma for environmentally relevant oxidation reactions. Their work emphasized that plasma methods enable controlled incorporation of active phases without significantly altering the structural integrity of the fibrous supports. The resulting catalysts displayed enhanced surface dispersion of transition metal oxides and improved catalytic behavior in oxidation reactions, reinforcing the potential of plasma-assisted functionalization for the design of advanced structured catalysts.

Biomorphic fibrous catalysts represent a powerful platform for the design of advanced oxidation catalysts, combining structural advantages with enhanced redox functionality. Their ability to integrate hierarchical architecture with tunable chemical composition makes them particularly attractive for applications under realistic operating conditions. Table 1 shows a comparison of temperatures indicative of the catalytic activity of different biomorphic fiber-based catalysts for the oxidation reactions of CO, benzene, and soot. It should be noted that the catalytic activity values compiled in Table 1 and in the following tables were obtained from independent studies employing different experimental protocols. Parameters such as reactant concentration, gas flow rate, catalyst loading, catalyst-to-soot ratio, reactor configuration, and heating rate may influence the reported T_{50} and T_M values. Therefore, the data are intended to provide a comparative overview of catalyst performance trends, and direct quantitative comparison between different studies should be interpreted with caution.

Table 1. Comparison of the activity of biomorphic fibers with different pollutant oxidations.

Catalyst	Oxidation Reaction	T_{50} (T_M) [a] (°C)	Conditions	Reference
Co fibers	Soot oxidation	(365)	NO (0.1%), O_2 (18%)/He Total flow 20 mL/min soot:catalyst mass ratio = 1:20	[95]
Ce fibers		(420)		
Co/Ce fibers		(380)		
Ce fibers	Soot oxidation	(442)	O_2 (3.33%), Ar (33.3%)/He Total flow 30 mL/min soot:catalyst mass ratio = 1:20	[97]
Co/Ce fibers		(414)		
Mn/Ce fibers		(424)		
Ce fibers	Benzene oxidation	379	Benzene (200 ppm), O_2 (10%)/He Total flow 100 mL/min	
Co/Ce fibers		277		
Mn/Ce fibers		235		
Ce fibers	Soot oxidation	(457)	NO (0.1%), O_2 (18%)/He Total flow 20 mL/min soot:catalyst mass ratio = 1:20	[98]
Mn fibers		(431)		
Mn,Ce fibers		(428)		
Mn,Ce,Co fibers		(420)		
Mn,Ce fibers	CO oxidation	275	CO (1%), O_2 (2%)/He Total flow 30 mL/min	
Mn,Ce,Co fibers		254		
Zr fibers	Soot oxidation	(537)	O_2 (3.33%), Ar (33.3%)/He Total flow 30 mL/min soot:catalyst mass ratio = 1:20	[99]
Mn/Zr fibers		(493)		
Fe/Zr fibers		(538)		
Zr fibers	CO oxidation	500	CO (1%), O_2 (2%)/He Total flow 30 mL/min	
Mn/Zr fibers		213		
Fe/Zr fibers		514		

[a] Values in parentheses correspond to T_M (temperature of maximum soot combustion rate) when T_{50} was not reported in the original reference.

5.1.2. Electrospun Fibrous Catalysts

The electrospinning method involves applying a high voltage to a polymer solution (polymer + ceramic precursor) in order to deform and draw the polymeric fluid from a nozzle or injector toward a collection surface. As it travels toward the collector, the solvent evaporates and solid nanofibers are deposited (Figure 7a). This method is relatively expensive because it requires specialized equipment, but it has many advantages over others: high reproducibility, the ability to produce individual fibers with smaller diameters (nanoscale), greater lengths, and a well-defined morphology.

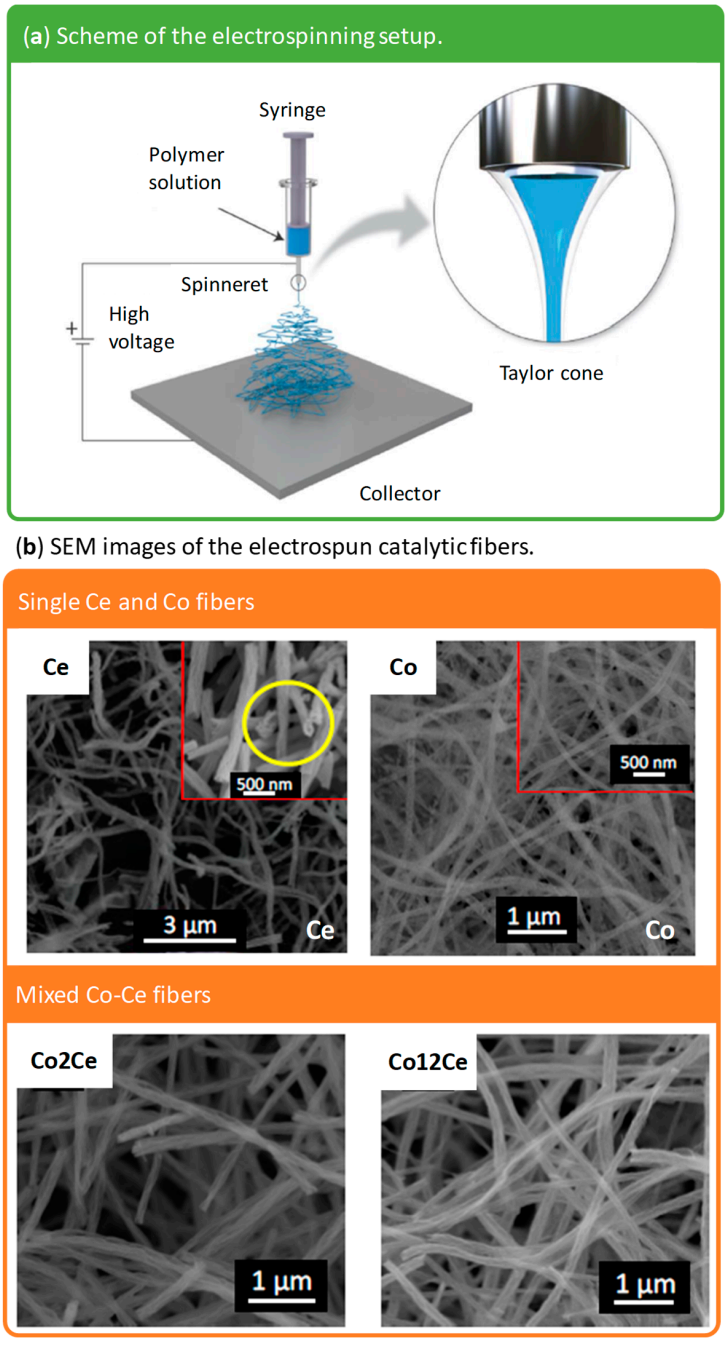

Figure 7. Electrospun fibers synthesized by Stegmayer [100]. (**a**) Schematic diagram of the device used in the synthesis of ceramic fibers via the electrospinning method. (**b**) SEM images of bulk electrospun fibers (cerium oxide fibers left and cobalt oxide fibers right) and cobalt-supported cerium oxide fibers with different cobalt loadings: 2 wt.% (**left**) and 12 wt. % (**right**). The yellow circle shows that the fibers are hollow.

Electrospinning has emerged as a versatile and effective method for the preparation of ceramic nanofibers with applications in environmental catalysis, particularly in oxidation reactions such as CO oxidation and diesel soot combustion. The technique enables the fabrication of one-dimensional nanostructures with high surface area, interconnected porosity, and tunable morphology. As highlighted in the review by Wu et al. [101], electrospun ceramic nanofibers combine structural stability with improved mass and heat transfer properties, making them attractive candidates for catalytic applications involving gas-phase oxidation reactions.

Recent studies have demonstrated that electrospun mixed oxides and perovskite-type materials exhibit remarkable catalytic performances due to synergistic redox interactions and defect-rich structures. Stegmayer et al. [102] reported the synthesis of Co_3O_4, CeO_2, and mixed Co–Ce oxide nanofibers via electrospinning (Figure 7b) and demonstrated their excellent activity toward both CO oxidation and diesel soot combustion. The enhanced performance of the mixed oxide fibers was associated with improved reducibility and oxygen exchange capacity arising from the interaction between cobalt and cerium species. Similarly, Liao et al. [103] investigated electrospun Ce–Mn oxide nanofibers for soot oxidation and showed that the combination of cerium and manganese promoted oxygen vacancy formation and facilitated lattice oxygen participation during combustion. Their work also emphasized the importance of the fibrous morphology in improving soot–catalyst contact efficiency.

The catalytic behavior of electrospun ceria-based fibers has also been explored in low-temperature CO oxidation. Sim et al. [104] demonstrated that doped CeO_2 electrospun fibers exhibited enhanced catalytic activity due to increased oxygen defects and improved oxygen mobility generated by aliovalent substitution in the ceria lattice. These structural modifications lowered the activation temperature for CO oxidation and highlighted the importance of defect engineering in electrospun oxide catalysts.

Perovskite nanofibers prepared by electrospinning have also shown promising oxidation properties. Ma et al. [105] synthesized $La_{0.8}Ce_{0.2}Fe_{1-x}Ni_xO_3$ nanofibers and observed that Ni incorporation significantly improved CO oxidation activity by increasing surface adsorbed oxygen species and catalyst reducibility. The fibrous morphology contributed to higher accessibility of active sites and facilitated gas diffusion, reinforcing the advantages of electrospun structures over conventional particulate catalysts.

In a related work, Stegmayer et al. [106] investigated cobalt deposited on ceria and zirconia micro- and nanostructures, including electrospun hollow ceria fibers, for diesel soot combustion. The study demonstrated that nanostructured fibrous supports enhanced cobalt dispersion and promoted oxygen transfer processes, resulting in improved catalytic performance compared with bulk materials. The authors highlighted the relevance of hierarchical morphology and strong metal–support interactions in soot oxidation catalysts.

From a broader perspective, the reviews by Wu et al. and Guerrero-Pérez [101,107] summarize the rapid development of electrospun nanofibers in catalysis and emphasize that their unique structural characteristics—including high aspect ratio, open porosity, interconnected networks, and tunable composition—provide significant advantages in oxidation catalysis.

Guerrero-Pérez particularly noted that electrospinning allows the rational design of multifunctional catalytic systems with controlled defect chemistry, enhanced redox properties, and improved thermal stability, which are key factors for environmental applications involving oxidation reactions.

These studies demonstrate that electrospinning is not only a powerful synthesis route for ceramic nanofibers but also a strategic tool for tailoring catalytic properties through morphology control, compositional tuning, and defect engineering. The combination of

fibrous architecture with redox-active oxides such as CeO_2, Co_3O_4, MnOx, and perovskites has proven particularly effective for oxidation reactions relevant to environmental catalysis. Table 2 shows a comparison of the temperatures indicative of the catalytic activity of different fiber-based catalysts produced by electrospinning for the oxidation reactions of CO and soot.

Table 2. Comparison of the activity of electrospun fibers with different pollutant oxidations.

Catalyst	Oxidation Reaction	T_{50} (T_M) [a] (°C)	Conditions	Reference
Co fibers	Soot oxidation	(380)	NO (0.1%), O_2 (18%)/He Total flow 20 mL/min soot:catalyst mass ratio = 1:20	[102]
Ce fibers		(380)		
Co,Ce fibers		(360)		
Co fibers	CO oxidation	150	CO (1%), O_2 (2%), He Total flow 30 mL/min	
Ce fibers		325		
Co,Ce fibers		175		
Mn fibers	Soot oxidation	439	O_2 (1%)/N_2 Total flow 100 mL/min soot:catalyst mass ratio = 1:10	[103]
Ce fibers		394		
Ce,Mn fibers		376		
Cu,Ce fibers	CO oxidation	52	CO (1%), O_2 (2%), N_2 Total flow 100 mL/min	[104]
Ni,Ce fibers		99		
Co,Ce fibers		131		
Mn,Ce fibers		131		
Fe,Ce fibers		192		
La,Ce fibers		311		
$La_{0.8}Ce_{0.2}Fe_{0.8}Ni_{0.2}O_3$	CO oxidation	214	CO (1%), O_2 (20%)/Ar Total flow 100 mL/min	[105]

[a] Values in parentheses correspond to T_M (temperature of maximum soot combustion rate) when T_{50} was not reported in the original reference.

5.2. Macrostructured Catalytic Supports for Oxidation Reactions

5.2.1. Monolithic Structures

Monoliths have emerged as highly attractive catalyst supports for CO, VOCs, and soot oxidation reactions due to their unique structural and transport properties. One of their main advantages is the low pressure drop associated with their parallel channel geometry, which enables the treatment of large gas flow rates with reduced energy consumption. In addition, monoliths provide a high geometric surface area and a uniform flow distribution, promoting efficient gas–solid contact and improved accessibility to the active catalytic sites.

Another important feature is their enhanced heat and mass transfer properties. The open-channel architecture facilitates reactant diffusion and heat dissipation, minimizing the formation of hot spots during highly exothermic oxidation reactions. Moreover, monolithic supports exhibit excellent thermal and mechanical stability, allowing operation under harsh reaction conditions and repeated thermal cycles without significant structural degradation.

Compared with powdered or pelletized catalysts, monoliths are easier to handle and integrate into continuous-flow reactors, while also reducing catalyst loss and secondary contamination due to the immobilization of the active phase on the structured support.

In CO oxidation, monolithic catalysts favor lower light-off temperatures and stable operation under continuous gas streams because of the efficient dispersion of active species and rapid heat transfer. For VOC oxidation, the high contact efficiency between gaseous pollutants and catalytic sites contributes to enhanced conversion efficiencies at lower operating temperatures and reduced energy demand. In soot oxidation, porous and

hierarchical monoliths improve soot–catalyst contact, which is one of the key limitations of this reaction, while also offering excellent thermal resistance during regeneration processes.

Monolithic catalysts offer an effective alternative to conventional particulate systems for emission control applications, as they combine low pressure drop, and high thermal stability. Commercial cordierite monoliths have been the most extensively studied systems. However, recent research has focused on the development of alternative monolithic structures, such as 3D-printed ceramic supports, for oxidation reactions.

Advances in fabrication methods, particularly 3D printing technologies, have enabled the development of tailored monolithic architectures with controlled porosity, channel geometry, and hierarchical structures, leading to improved catalytic performance.

Printed 3D Monoliths

Three-dimensional (3D) printing appears as a powerful manufacturing strategy for the preparation of structured monolithic catalysts for environmental oxidation reactions. Compared with conventional honeycomb monoliths, 3D-printed catalytic structures offer control over geometry, channel architecture, porosity, and mass transfer properties, enabling the optimization of catalytic performance and pressure drop. In addition, additive manufacturing allows the fabrication of complex and highly accessible structures that improve heat transfer and reactant distribution during oxidation processes such as CO oxidation, VOC abatement, and soot combustion.

Courtalón et al. [108] developed clay-based monolithic supports fabricated by Direct Ink Writing (DIW) 3D printing using a woodpile-type geometry specifically designed for catalytic applications. These structures exhibited suitable mechanical resistance and structural stability, with properties comparable to or even superior to those of commercial cordierite monoliths. The active phase, composed of Co and Ce oxides, was incorporated by impregnation using precursor solutions with different concentrations. The authors observed that catalytic performance depended not only on the amount of active phase deposited, but also on its spatial distribution and accessibility within the 3D-printed structure. The heterogeneous deposition and accumulation of active species on the filament surface reduced reactant diffusion and the access to internal catalytic sites. Among the evaluated samples, the monoliths impregnated using the lowest precursor concentration exhibited the highest catalytic activity for soot combustion.

Bueno-López and co-workers [109] employed 3D-printing technology to fabricate templates for the preparation of cordierite honeycomb monoliths with asymmetric channel geometries designed to enhance the performance of conventional catalytic supports. In these structures, the channel cross-section is wider at the inlet and progressively decreases toward the outlet, favoring both reaction kinetics and mass transfer phenomena. Compared with traditional monoliths, the asymmetric design improved catalytic performance under kinetic control conditions and enhanced radial diffusion when external gas-phase diffusion limitations became significant. To demonstrate the applicability of this concept, Cu/CeO_2 catalysts deposited onto both conventional and asymmetric monoliths were evaluated in CO oxidation under oxygen-rich conditions and in preferential CO oxidation (CO-PrOx) in H_2-rich streams, reactions that are highly relevant for environmental remediation and fuel cell technologies, respectively.

In a recent work [110], a layered porous monolithic OM-SiO_2 substrate was synthesized by 3D printing ink direct writing technology, and then Co-MOFs were encapsulated into the monolithic catalyst substrate by a vacuum self-assembly method. The authors studied the developed printed monolith to the catalytic oxidation of toluene. They found that the monolithic catalyst showed a good performance towards the VOC oxidation, aiming that the combination of the 3D printing technology with the MOFs structure exhibit the

advantages of ordered mesoporous materials with active species to form macro-layered porous materials and provide ideas and an experimental basis for the elimination of VOCs in industrial applications.

3D-printed monolithic catalysts represent a promising next-generation technology for environmental catalysis. Their tunable structure, scalability, and compatibility with a wide range of catalytic materials provide significant opportunities for the development of efficient oxidation systems with improved heat and mass transfer characteristics. Figure 8a shows photographs and SEM micrographs of structures printed using 3D printing technology while Figure 8b shows SEM/EDS images of printed 3D microarchitectures of inorganic porous materials.

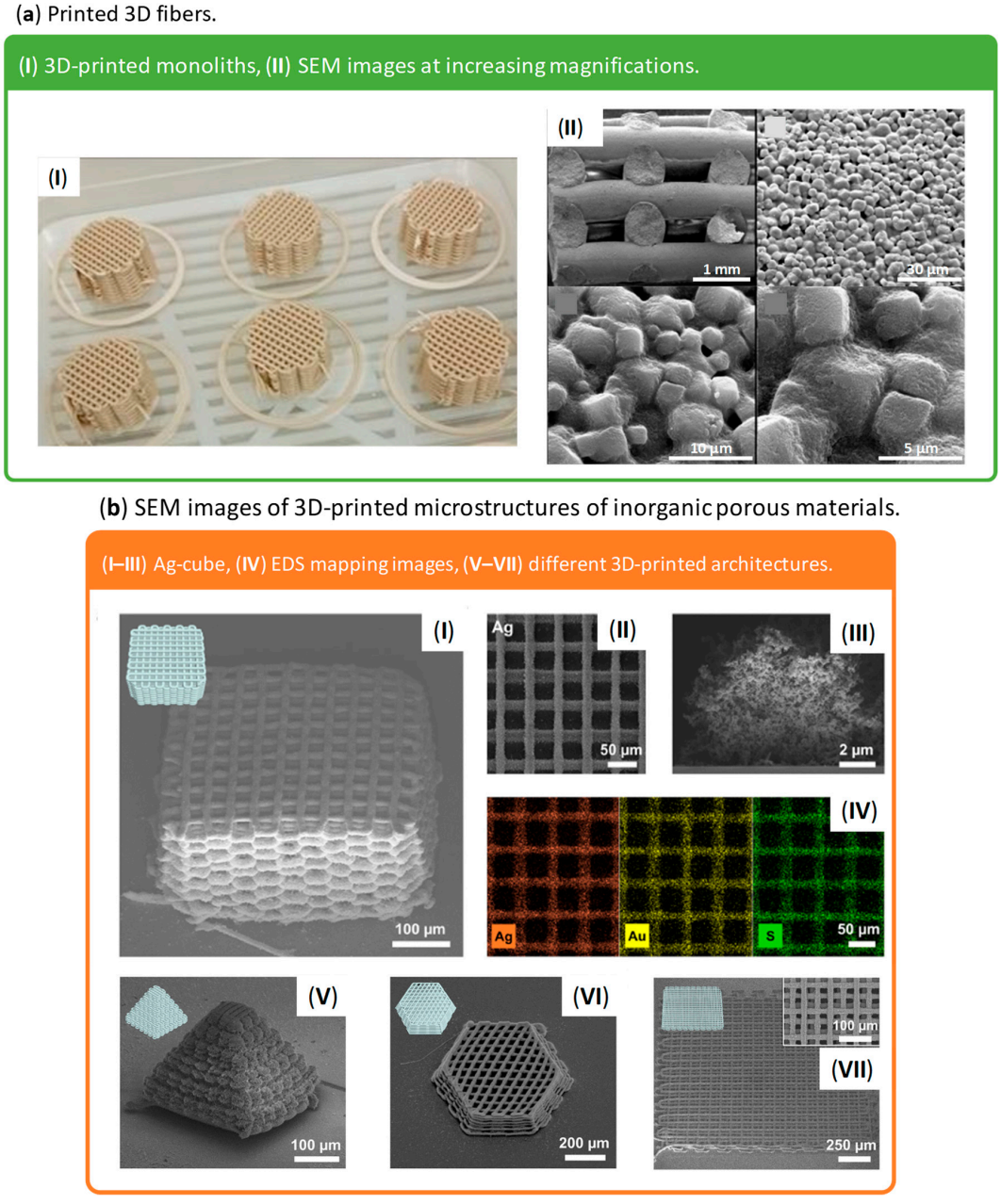

Figure 8. Photografs and micrographs of 3D-printed monoliths. (**a**), Adapted from [111], Figures 2 and 4, https://doi.org/10.3390/catal14010085, licensed under CC BY 4.0 (https://creativecommons.org/licenses/by/4.0, accessed on 28 June 2026). (**b**), Adapted from [112], Figure 2, https://doi.org/10.1038/s41467-023-44145-7, licensed under CC BY 4.0 (https://creativecommons.org/licenses/by/4.0, accessed on 28 June 2026).

Wire Mesh Monoliths

Stacked wire mesh monoliths constitute an attractive alternative to conventional ceramic monoliths and particulate filters for environmental catalytic applications, particularly in oxidation reactions involving diesel soot, carbon monoxide, and volatile organic compounds (VOCs). These structured systems are based on the assembly of metallic woven meshes arranged in stacked configurations, providing high mechanical resistance, enhanced heat transfer, low pressure drop, and excellent accessibility of the catalytic active phase. Their open structure also facilitates gas diffusion and promotes improved contact between soot particles and catalytic surfaces, which is especially advantageous for diesel exhaust treatment. Figure 9a shows photographs illustrating the assembly of metal meshes inside a cartridge and various cartridges assembled using meshes with different mesh sizes.

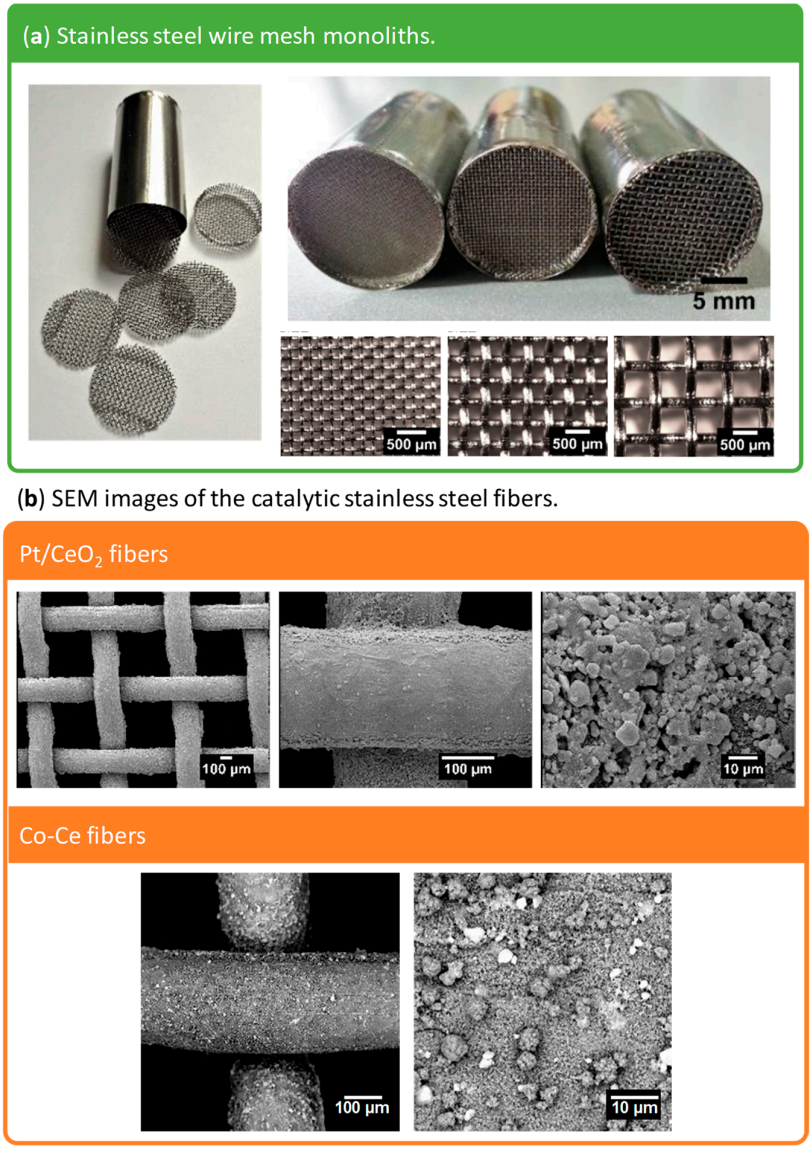

Figure 9. Stainless steel wire mesh monoliths developed by Godoy [113]. (**a**) Photograph of an unassembled cartridge showing the inner mesh (**left**). Assembled metal cartridges containing stainless steel mesh with different mesh sizes (**right**). (**b**) SEM images of the central mesh of a cartridge coated with a layer of CeO_2, onto which Pt (**top** images) or Co_3O_4 (**bottom** images) was impregnated.

One of the earliest studies on this topic was reported by Godoy et al. [113], who investigated stacked wire mesh monoliths for the simultaneous abatement of VOCs (n-

hexane, ethyl acetate and toluene) and diesel soot. The authors demonstrated that the metallic mesh architecture allowed the efficient deposition of catalytic phases, composed of Co,Ce oxides, while maintaining a highly permeable structure. The monolithic arrangement favored both gaseous pollutant oxidation and soot combustion due to improved mass transfer and reduced diffusional limitations compared with conventional packed systems. In addition, the metallic substrate contributed to enhanced thermal conductivity, facilitating temperature homogenization during catalytic operation. This means stacked wire mesh structures disposed into a convenient cartridge can be considered as versatile catalytic supports for multifunctional environmental applications.

Subsequent research focused on optimizing the cartridge configuration of these structured catalysts. In their study on single- and double-bed stacked wire mesh cartridges, Godoy et al. [113] evaluated different monolith arrangements for the catalytic treatment of diesel exhausts. The authors observed that double-bed configurations improved catalytic performance by increasing the interaction between particulate matter and the active catalytic surfaces. The structured geometry also allowed flexible catalyst design while maintaining relatively low pressure drop, which is a critical parameter for practical exhaust treatment systems. The work highlighted the importance of monolith architecture in balancing filtration efficiency, catalytic activity, and fluid dynamic behavior. Figure 9b shows SEM micrographs of metal meshes coated with Pt,Ce and Co,Ce catalysts.

Further advances were achieved through scaling-up studies aimed at evaluating the applicability of stacked wire mesh filters under more realistic operating conditions. Godoy et al. [114] demonstrated that catalytic stacked wire mesh filters could be successfully scaled up while preserving their favorable catalytic and hydrodynamic properties. The scaled systems maintained efficient soot oxidation activity and acceptable pressure drop values, confirming the feasibility of this technology for larger-scale diesel exhaust applications. The study emphasized that the intrinsic thermal conductivity of metallic meshes contributed to improved heat distribution throughout the monolith, promoting more uniform catalytic performance and regeneration behavior.

More recently, Godoy et al. [115] investigated the deposition of Co–Ce oxide nanoparticles synthesized by an aerosol-assisted method onto different structured substrates, including stacked wire mesh monoliths, for diesel particulate matter removal. The aerosol synthesis route enabled the preparation of highly dispersed mixed oxide nanoparticles with enhanced redox properties and oxygen mobility. When deposited on stacked wire mesh supports, the Co–Ce catalysts exhibited remarkable soot oxidation activity due to the synergistic interaction between cobalt and cerium species, which promoted oxygen transfer processes and improved catalyst reducibility. The study also compared different structured substrates and demonstrated that stacked wire mesh monoliths provided advantageous characteristics in terms of catalyst accessibility, soot–catalyst contact, and thermal management.

Collectively, these studies demonstrate that stacked wire mesh monoliths constitute a highly promising structured catalyst technology for oxidation reactions of environmental relevance. Their open metallic architecture combines low pressure drop with high heat and mass transfer efficiency, while allowing flexible incorporation of catalytically active phases such as Co–Ce mixed oxides. Moreover, the possibility of tailoring mesh arrangement, cartridge geometry, and catalyst deposition strategies provides significant opportunities for optimizing CO oxidation, soot combustion, VOC oxidation, and diesel exhaust treatment systems. The scalability and robustness of these monolithic structures further support their potential for practical industrial and automotive applications.

Table 3 shows a comparison of the temperatures indicative of the catalytic activity of different monolithic catalysts for the oxidation reactions of CO, toluene, and soot.

Table 3. Comparison of the activity of monolithic catalysts with different pollutant oxidations.

Catalyst Washcoated on Monoliths	Oxidation Reaction	T_{50} ™ [a] (°C)	Conditions	Reference
Co,Ce—3D ceramic monolith	Soot oxidation	389	NO (0.1%), O_2 (18%)/He Total flow 20 mL/min impregnated by a 600 ppm soot suspension in hexane	[108]
Cu,Ce—3D Al_2O_3 monolith	CO oxidation	- [b]	CO (1%), O_2 (17%)/He Total flow 400 mL/min	[109]
Co_3O_4@SiO_2—3D SiO_2 monolith	Toluene oxidation	276	Toluene (300 ppm) Total flow 200 mL/min	[110]
Pt,Ce—wire mesh monolith	Soot oxidation	(442)	NO (0.1%), O_2 (18%)/He Total flow 20 mL/min impregnated by a 600 ppm soot suspension in n-hexane	[113]
Pt,Ce—wire mesh monolith	Soot oxidation	(436)	NO (0.1%), O_2 (18%)/He Total flow 20 mL/min impregnated by a 600 ppm soot suspension in ethyl acetate	
Pt,Ce—wire mesh monolith	Soot oxidation	(433)	NO (0.1%), O_2 (18%)/He Total flow 20 mL/min impregnated by a 600 ppm soot suspension in toluene	
Pt,Ce + Co,Ce—wire mesh monolith	Soot oxidation	(409)	NO (0.1%), O_2 (18%)/He Total flow 20 mL/min impregnated by a 600 ppm soot suspension in n-hexane	
Pt,Ce + Co,Ce—wire mesh monolith	Soot oxidation	(396)	NO (0.1%), O_2 (18%)/He Total flow 20 mL/min impregnated by a 600 ppm soot suspension in ethyl acetate	
Pt,Ce + Co,Ce—wire mesh monolith	Soot oxidation	(394)	NO (0.1%), O_2 (18%)/He Total flow 20 mL/min impregnated by a 600 ppm soot suspension in toluene	
Co Nps,Ce—wire mesh monolith	Soot oxidation	(417)	NO (0.1%), O_2 (18%)/He Total flow 20 mL/min impregnated by a 600 ppm soot suspension in hexane	[115]

[a] Values in parentheses correspond to T_M (temperature of maximum soot combustion rate) when T_{50} was not reported in the original reference. [b] T_{50} was not reported in the original reference. Catalytic activity was reported as a reaction rate of 0.2 µmol $CO \cdot s^{-1} \cdot gcat^{-1}$ at 77 °C, calculated from CO conversion values lower than 15%.

5.2.2. Ceramic Papers as Structured Catalysts: Preparation Strategies and Catalytic Performance

Ceramic papers have emerged as a versatile class of structured catalysts for oxidation processes, combining the advantages of fibrous materials with tunable catalytic functionality.

Their three-dimensional network, formed by interconnected ceramic fibers, provides high external surface area, low pressure drop, and enhanced mass and heat transfer, making them particularly suitable for gas-phase reactions and applications involving particulate matter such as diesel soot [88]. Figure 10a shows photographs and an X-ray tomogram of ceramic papers.

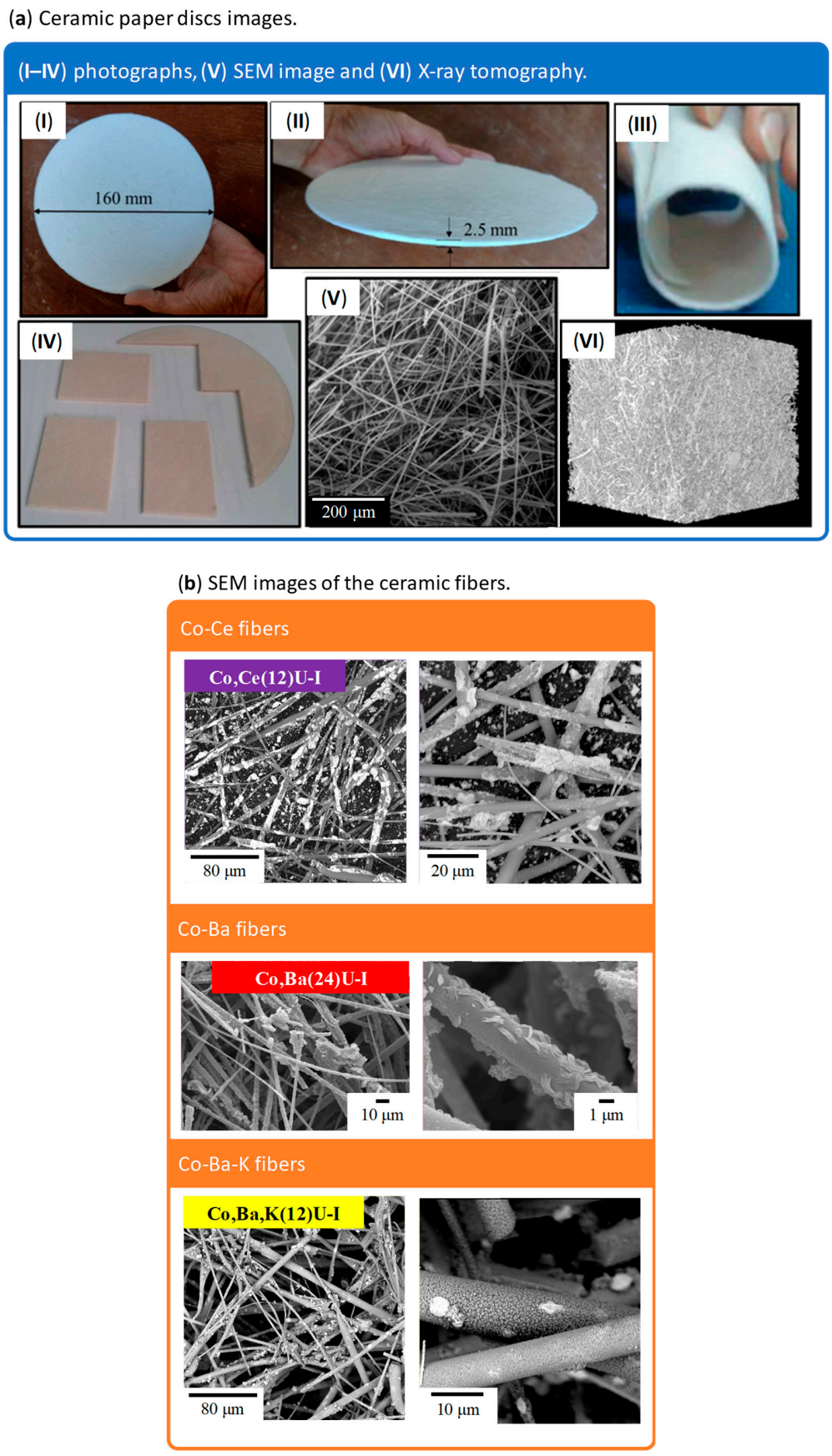

Figure 10. Ceramic fibers structured as ceramic papers [88,116]. (**a**) Images that show the flexibility and porosity of ceramic papers. (**b**) Micrographs of SiO_2-Al_2O_3 ceramic papers loaded with either cobalt + cerium, cobalt + barium or cobalt + barium + potassium catalysts.

The synthesis of paper-based ceramic catalysts generally involves a two-step process. First, a fibrous matrix is fabricated through a papermaking-like procedure in which ceramic fibers, typically based on SiO_2–Al_2O_3 compositions with high thermal resistance (up to approximately 900 °C), are combined with binders to produce a mechanically stable structure [88,116]. The choice of binder plays a crucial role not only in determining the mechanical integrity of the material, but also in influencing its catalytic performance. For example, cerium oxide-based binders provide intrinsic redox functionality, contributing to oxygen storage capacity and enabling catalytic activity even in the absence of additional active phases [117,118]. Natural borates represent another class of binders; they are directly extracted from mineral deposits and subsequently purified, offering the advantages of low cost and wide availability. Although they do not exhibit intrinsic catalytic activity, ceramic papers prepared with natural borates show greater mechanical strength than those fabricated using CeO_2 colloidal suspension as binders [88,117]. The resulting structure consists of a porous network with interconnected voids that facilitate gas diffusion and improve accessibility to active sites.

In the second stage, the catalytic phase is incorporated using techniques such as wet spraying [118], dry spraying [119], or drip impregnation [88,116]. These methods strongly influence the dispersion, localization, and accessibility of the active species. In particular, solvent properties, especially surface tension, govern the penetration depth of precursor solutions and the resulting particle size distribution. Low-surface-tension solvents favor the homogeneous deposition of finely dispersed particles on the fiber surfaces, whereas aqueous systems tend to promote deeper penetration and the formation of larger aggregates within the bulk structure. This distinction has important implications for catalytic performance, since surface-localized species are generally more active under controlled laboratory conditions, while bulk-distributed catalysts may become advantageous under realistic operating conditions where reactants penetrate the entire fibrous structure.

Sacco et al. [118] reported the deposition of Co and Ce catalytic phases onto ceramic papers by wet spraying. They found that the use of alcoholic solutions for cobalt impregnation produced smaller particles and a more homogeneous dispersion over the ceramic fibers compared with aqueous solutions. In a later study, Sacco et al. [120] demonstrated that the incorporation of citric acid into Mn–Ce precursor solutions improved the distribution of the catalytic phase on the ceramic fibers, leading to enhanced catalytic performance in all the evaluated systems, with the equimolar Mn–Ce mixed oxide showing the highest activity.

Similarly, Tuler et al. [119] proposed a dry-spray impregnation method to improve the catalytic properties of ceramic papers used as catalytic filters for diesel soot removal. This method enabled the efficient and homogeneous deposition of small Co and Ce oxide particles, which acted as active sites for soot combustion. In contrast, conventional drip impregnation produced larger agglomerates preferentially located at the intersections between ceramic fibers. Consequently, spray-coated catalytic papers exhibited superior performance, reducing soot combustion temperatures by approximately 30 °C.

More recently, Leonardi et al. [88] investigated drip impregnation and showed that catalytic activity depended not only on metal loading, but mainly on achieving homogeneous coverage and dispersion of the active phase over the ceramic fiber surface. Under these conditions, Co–Ba–K catalysts exhibited better performance than Co–Ce systems (Figure 10b), particularly at loadings of 12 wt.% relative to the fiber mass. Catalytic performance is highly dependent on both composition and loading of the active phase. Low loadings (≈5 wt.%) generally result in limited improvements compared to the bare support, whereas intermediate loadings (12–24 wt.%) significantly enhance activity, reducing soot combustion temperatures by more than 100 °C in some systems.

Beyond composition, the intrinsic structure of ceramic papers plays a decisive role in catalytic performance. Their fibrous network promotes intimate contact between catalyst and soot particles, addressing one of the main limitations in soot oxidation processes. Simultaneously, the interconnected porosity enhances gas diffusion and heat transfer, contributing to improved reaction kinetics. This combination of structural and chemical features enables ceramic papers to function not only as catalysts but also as filtration media, integrating multiple functionalities within a single material.

Table 4 shows a comparison of the temperatures representative of the catalytic activity of catalytic ceramic papers prepared by different methods for the soot oxidation reaction.

Table 4. Comparison of the activity of catalytic ceramic papers to soot oxidation. Conditions: NO (0.1%), O_2 (18%)/He. Total flow: 20 mL/min. Soot impregnated by a 600 ppm soot suspension in hexane.

Catalyst Impregnated on SiO_2-Al_2O_3 Ceramic Papers (CP)	Impregnation Method	T_{50} (T_M) [a] (°C)	Reference
Co(W)—CP	Wet spray	408	[118]
Co(I)—CP	Wet spray	381	
Mn,Ce(CA)—CP	Wet spray	(392)	[120]
Mn,Ce(W)—CP	Wet spray	(440)	
20-Ce-Ce-Co-S600	Dry spray	(450)	[119]
20-Ce-Ce-Co-I600	drip	(480)	
Co,Ce(5)U-I	drip	(560)	[88]
Co,Ce(12)U-I	drip	(440)	
Co,Ce(24)U-I	drip	(410)	
Co,Ba,K(5)U-I	drip	(500)	
Co,Ba,K(12)U-I	drip	(410)	
Co,Ba,K(24)U-I	drip	(410)	

[a] Values in parentheses correspond to T_M (temperature of maximum soot combustion rate) when T_{50} was not reported in the original reference.

Ceramic papers represent a highly adaptable platform in which catalytic performance can be tuned through the interplay of synthesis parameters, structural design, and active phase composition. Their ability to bridge intrinsic catalytic properties with macroscopic transport phenomena makes them particularly attractive for applications requiring efficient oxidation under realistic conditions, such as emission control systems.

6. Conclusions

Catalytic oxidation remains one of the most effective technologies for the abatement of carbon monoxide (CO), volatile organic compounds (VOCs), and diesel soot because it enables high conversion efficiencies under relatively mild operating conditions. This review demonstrates that the performance of oxidation catalysts is dictated by the interplay between reaction mechanisms, oxygen mobility, oxygen vacancies, redox behavior, metal–support interactions, and catalyst composition. Although noble metals continue to deliver outstanding low-temperature activity, transition metal oxides, mixed oxides, and perovskite-type materials have emerged as attractive and more sustainable alternatives owing to their abundant lattice oxygen, high oxygen storage capacity, and tunable defect chemistry.

Beyond catalyst composition, this review highlights the growing importance of catalyst architecture in determining practical performance. Structured catalysts—including biomorphic fibers, electrospun nanofibers, catalytic ceramic papers, conventional monoliths, and additively manufactured (3D-printed) monoliths—improve heat and mass transfer, reduce pressure drop, and enhance catalyst accessibility. When combined with mechanistic understanding and reliable kinetic models, these structured systems provide an effective pathway for translating laboratory-scale catalysts into high-performance reactor configurations for environmental applications.

Despite these significant advances, important barriers still limit large-scale industrial implementation. Long-term catalyst durability remains a critical challenge because thermal aging, sulfur and water poisoning, carbon deposition, sintering, and structural degradation progressively reduce catalytic activity. Moreover, successful commercialization requires more than high intrinsic activity; catalysts must also exhibit mechanical robustness, reproducible manufacturing, regeneration capability, cost-effective production, and stable operation under realistic and fluctuating process conditions. Addressing these requirements demands a closer integration of catalyst development with reactor engineering and process design.

Several research directions are expected to drive the next generation of catalytic oxidation technologies. Machine learning and other data-driven methodologies offer new opportunities to accelerate catalyst discovery by identifying relationships between composition, defect chemistry, synthesis parameters, and catalytic performance. At the same time, advanced in situ and operando characterization techniques will provide unprecedented insight into oxygen vacancy dynamics, lattice oxygen participation, oxidation-state changes, and catalyst restructuring under reaction conditions, enabling a more rational design of oxidation catalysts. In parallel, scaling up structured catalytic systems laboratory prototypes to pilot-scale and industrial reactors will be essential to fully exploit their advantages in heat and mass transfer while ensuring manufacturing reproducibility, mechanical integrity, and long-term stability.

This review underscores that the future of catalytic oxidation lies not in optimizing isolated catalyst properties, but in integrating mechanistic understanding, catalyst chemistry, structured catalyst engineering, advanced manufacturing technologies, and reactor design into a unified framework. Such an approach will facilitate the development of robust, efficient, and economically viable catalytic systems capable of meeting increasingly stringent environmental regulations while supporting sustainable industrial pollution control.

Author Contributions: Conceptualization, S.A.L., E.E.M. and V.G.M.; methodology, S.A.L. and M.L.G.; software, S.A.L. and M.L.G.; validation, S.A.L., and V.G.M.; formal analysis, E.E.M. and V.G.M.; investigation, S.A.L. and V.G.M.; resources, V.G.M. and E.E.M.; data curation, S.A.L. and M.L.G.; writing—original draft preparation, S.A.L., M.L.G. and V.G.M.; writing—review and editing, S.A.L. and V.G.M.; visualization, S.A.L. and V.G.M.; supervision, V.G.M. and E.E.M.; project administration, V.G.M. and E.E.M.; funding acquisition, V.G.M. and E.E.M. All authors have read and agreed to the published version of the manuscript.

Funding: This research was funded by Universidad Nacional del Litoral (UNL) grant number CAI+D 2024, and Consejo Nacional de Investigaciones Científicas y Técnicas (CONICET) grant number PIP-0689.

Data Availability Statement: No new data were created or analyzed in this study. Data sharing is not applicable to this article.

Acknowledgments: The authors acknowledge the financial support provided by the Agencia Nacional de Promoción Científica y Tecnológica (ANPCyT), Consejo Nacional de Investigaciones Científi-

cas y Técnicas (CONICET), Secretaría de Ciencia y Tecnología e Innovación (SeCTeI) and Universidad Nacional del Litoral (UNL).

Conflicts of Interest: The authors declare no conflict of interest.

References

1. Kembo, J.P.N.; Wang, J.; Luo, N.; Gao, F.; Yi, H.; Zhao, S.; Zhou, Y.; Tang, X. A review of catalytic oxidation of carbon monoxide over different catalysts with an emphasis on hopcalite catalysts. *New J. Chem.* **2023**, *47*, 20222–20247. [CrossRef]
2. Zheng, Y.; Xu, W.; Yang, J.; Shan, C.; Wang, Y.; Han, R.; Zang, G.; Liu, Q. Catalytic oxidation of VOCs and CO on cobalt-based Materials: Strategies and mechanisms for improving activity and stability. *Chem. Eng. J.* **2024**, *484*, 149296. [CrossRef]
3. Yi, J.; Liu, J.; Gao, B.; Bo, L.; Cao, L.; Sillanpää, M. The comprehensive review of catalysts for catalytic oxidation of volatile organic compounds. *J. Environ. Chem. Eng.* **2025**, *13*, 115691. [CrossRef]
4. Liu, R.; Wu, H.; Shi, J.; Xu, X.; Zhao, D.; Hau, Y.; Zhang, M.; Liu, S.; Ding, H. Recent progress on catalysts for catalytic oxidation of volatile organic compounds: A review. *Catal. Sci. Technol.* **2022**, *12*, 6945–6991. [CrossRef]
5. He, J.; Zheng, F.; Zhou, Y.; Li, X.; Wang, Y.; Xiao, J.; Li, Y.; Chen, D.; Lu, J. Catalytic oxidation of VOCs over 3D@2D Pd/$CoMn_2O_4$ nanosheets supported on hollow Al_2O_3 microspheres. *J. Colloid Interface Sci.* **2022**, *613*, 155–167. [CrossRef] [PubMed]
6. Prasad, R.; Singh, S.V. A review on catalytic oxidation of soot emitted from diesel fueled engines. *J. Environ. Chem. Eng.* **2020**, *8*, 103945. [CrossRef]
7. Huang, J.; Gao, J.; Liu, J.; Wang, X.; Tian, G.; Chen, H. A review of the application of soot catalysts: Focus on the soot oxidation-induced fragmentation process. *Energy Fuels* **2024**, *38*, 20057–20083. [CrossRef]
8. Fan, Z.; Gao, F.; Zhang, J.; Yi, L.; Luo, N.; Yi, H.; Tang, X. Advances in CO catalytic oxidation on typical metal oxide catalysts: Performance, mechanism, and optimization. *J. Mater. Chem. A* **2025**, *13*, 26129–26165. [CrossRef]
9. Kiani, D.; Wachs, I.E. Practical considerations for understanding surface reaction mechanisms involved in heterogeneous catalysis. *ACS Catal.* **2024**, *14*, 16770–16784. [CrossRef] [PubMed]
10. Zang, M.; Zhao, C.; Wang, Y.; Chen, S. A review of recent advances in catalytic combustion of VOCs on perovskite-type catalysts. *J. Saudi Chem. Soc.* **2019**, *23*, 645–654. [CrossRef]
11. Tong, Y.; Wang, S.; Yue, T. Progress in catalytic oxidation of noble metal-based carbon monoxide: Oxidation mechanism, sulfur resistance, and modification. *Catalysts* **2025**, *15*, 415. [CrossRef]
12. Teymoori, S.M.; Alavi, S.M.; Rezaei, M. Catalytic oxidation of CO over the MOx—Co_3O_4 (M: Fe, Mn, Cu, Ni, Cr, and Zn) mixed oxide nanocatalysts at low temperatures. *Sci. Rep.* **2025**, *15*, 25808. [CrossRef] [PubMed]
13. Zhao, R.; Wang, H.; Zhao, D.; Liu, R.; Liu, S.; Fu, J.; Zhang, Y.; Ding, H. Review on Catalytic Oxidation of VOCs at Ambient Temperature. *Int. J. Mol. Sci.* **2022**, *23*, 13739. [CrossRef]
14. Georgiou, Y.; Smyrnioti, M.; Ioannides, T. Co_3O_4 Catalysts for Complete Toluene Oxidation: Review including Meta-Analysis of Catalyst Activity Data. *Catalysts* **2023**, *13*, 1454. [CrossRef]
15. Xu, T.; Wang, C.; Lv, Y.; Zhu, B.; Zhang, X. Catalytic Oxidative Removal of Volatile Organic Compounds (VOCs) by Perovskite Catalysts: A Review. *Nanomaterials* **2025**, *15*, 685. [CrossRef] [PubMed]
16. Zhao, T.; Song, Z.; Wu, C.; Li, Y.; Li, H.; Wei, Y.; Yao, S.; Xiao, M.; Zhao, M.; Cui, B. Advancements in cobalt-based oxide catalysts for soot oxidation: Enhancing catalytic performance through modification and morphology control. *Smart Mol.* **2024**, *2*, e20240024. [CrossRef] [PubMed]
17. Sereewatthanawut, I.; Khajonvittayakul, C.; Swadchaipong, N.; Tongnan, V.; Maneesard, P.; Ampairojanawong, R.; Makdee, A.; Kangsadan, T.; Hartley, M.; Hartley, U.W. Enhanced catalytic performance of MnO_2 nanowires for soot combustion by cobalt incorporation. *Mater. Adv.* **2025**, *6*, 6416–6426. [CrossRef]
18. Colvile, R.N.; Hutchinson, E.J.; Mindell, J.S.; Warren, R.F. The transport sector as a source of air pollution. *Atmos. Environ.* **2001**, *35*, 1537–1565. [CrossRef]
19. Vallero, D.A. Environmental Impacts of Energy Production, Distribution and Transport. In *Future Energy: Improved, Sustainable and Clean Options for Our Planet*; Elsevier Inc.: Amsterdam, The Netherlands, 2013; pp. 551–581.
20. Speight, J.G. Combustion of hydrocarbons. In *Handbook of Industrial Hydrocarbon Processes*; Gulf Professional Publishing: Oxford, UK, 2011; Chapter 10; pp. 355–393.
21. Li, P.; Chen, X.; Li, Y.; Schwank, J.W. A review on oxygen storage capacity of CeO_2-based materials: Influence factors, measurement techniques, and applications in reactions related to catalytic automotive emissions control. *Catal. Today* **2019**, *327*, 90–115. [CrossRef]
22. United States Environmental Protection Agency (EPA). Basic Information About Carbon Monoxide Outdoor Air Pollution. Available online: https://www.epa.gov/co-pollution/basic-information-about-carbon-monoxide-co-outdoor-air-pollution (accessed on 9 July 2026).

23. Dey, S.; Dhal, G.C. Materials progress in the control of CO and CO_2 emission at ambient conditions: An overview. *Mater. Sci. Energy Technol.* **2019**, *2*, 607–623. [CrossRef]
24. Vohra, K.; Vodonos, A.; Schwartz, J.; Marais, E.A.; Sulprizio, M.P.; Mickley, L.J. Global mortality from outdoor fine particle pollution generated by fossil fuel combustion: Results from GEOS-Chem. *Environ. Res.* **2021**, *195*, 110754. [CrossRef] [PubMed]
25. Reis, H.; Reis, C.; Sharip, A.; Reis, W.; Zhao, Y.; Sinclair, R.; Beeson, L. Diesel exhaust exposure, its multi-system effects, and the effect of new technology diesel exhaust. *Environ. Int.* **2018**, *114*, 252–265. [CrossRef] [PubMed]
26. Platt, S.M.; El Haddad, I.; Pieber, S.M.; Zardini, A.A.; Suarez-Bertoa, R.; Clairotte, M.; Daellenbach, K.R.; Huang, R.-J.; Slowik, J.G.; Hellebust, S.; et al. Gasoline cars produce more carbonaceous particulate matter than modern filter-equipped diesel cars. *Sci. Rep.* **2017**, *7*, 4926. [CrossRef] [PubMed]
27. Kontses, A.; Triantafyllopoulos, G.; Ntziachristos, L.; Samaras, Z. Particle number (PN) emissions from gasoline, diesel, LPG, CNG and hybrid-electric light-duty vehicles under real-world driving conditions. *Atmos. Environ.* **2020**, *222*, 117126. [CrossRef]
28. Guan, B.; Zhan, R.; Lin, H.; Huang, Z. Review of the state-of-the-art of exhaust particulate filter technology in internal combustion engines. *J. Environ. Manag.* **2015**, *154*, 225–258. [CrossRef]
29. Mohankumar, S.; Senthilkumar, P. Particulate matter formation and its control methodologies for diesel engine: A comprehensive review. *Renew. Sustain. Energy Rev.* **2017**, *80*, 1227–1238. [CrossRef]
30. Adams, K.; Greenbaum, D.S.; Shaikh, R.; van Erp, A.M.; Russell, A.G. Particulate matter components, sources, and health: Systematic approaches to testing effects. *J. Air Waste Manag. Assoc.* **2015**, *65*, 544–558. [CrossRef] [PubMed]
31. Piumetti, M.; Bensaid, S. *Nanostructured Catalysts for Applications Environmental*; Springer International Publishing: Cham, Switzerland, 2021.
32. Bueno-López, A. Diesel soot combustion ceria catalysts. *Appl. Catal. B* **2014**, *146*, 1–11. [CrossRef]
33. Yang, C.; Miao, G.; Pi, Y.; Xia, Q.; Wu, J.; Li, Z.; Xiao, J. Abatement of various types of VOCs by adsorption/catalytic oxidation: A review. *Chem. Eng. J.* **2019**, *370*, 1128–1153. [CrossRef]
34. Kamal, M.S.; Razzak, S.A.; Hossain, M.M. Catalytic oxidation of volatile organic compounds (VOCs)—A review. *Atmos. Environ.* **2016**, *140*, 117–134. [CrossRef]
35. Guo, Y.; Wen, M.; Li, G.; An, T. Recent advances in VOC elimination by catalytic oxidation technology onto various nanoparticles catalysts: A critical review. *Appl. Catal. B* **2021**, *281*, 119447. [CrossRef]
36. Medium.Com. *Global Strategies for Mitigating Air Pollution and Preserving Public Health*; Medium.Com: San Francisco, CA, USA, 2023.
37. He, C.; Cheng, J.; Zhang, X.; Douthwaite, M.; Pattisson, S.; Hao, Z. Recent Advances in the Catalytic Oxidation of Volatile Organic Compounds: A Review Based on Pollutant Sorts and Sources. *Chem. Rev.* **2019**, *119*, 4471–4568. [CrossRef] [PubMed]
38. Zhang, F.; Gutiérrez, R.A.; Lustemberg, P.G.; Liu, Z.; Rui, N.; Wu, T.; Ramírez, P.J.; Xu, W.; Idriss, H.; Ganduglia-Pirovano, M.V.; et al. Metal–support interactions and C1 chemistry: Transforming Pt CeO_2 into a highly active and stable catalyst for the conversion of carbon dioxide and methane. *ACS Catal.* **2021**, *11*, 1613–1623. [CrossRef] [PubMed]
39. Trovarelli, A. Catalytic properties of ceria and CeO_2-containing materials. *Catal. Rev.* **1996**, *38*, 439–520. [CrossRef]
40. Morgan, K.; Maguire, N.; Fushimi, R.; Gleaves, J.T.; Goguet, A.; Harold, M.P.; Kondratenko, E.V.; Menon, U.; Schuurman, Y.; Yablonsky, G.S. Forty years of temporal analysis of products. *Catal. Sci. Technol.* **2017**, *7*, 2416–2439. [CrossRef]
41. Zaera, F. In-situ and operando spectroscopies for the characterization of catalysts and of mechanisms of catalytic reactions. *J. Catal.* **2021**, *404*, 900–910. [CrossRef]
42. Doornkamp, C.; Ponec, V. The universal character of the Mars and Van Krevelen mechanism. *J. Mol. Catal. A Chem.* **2000**, *162*, 19–32. [CrossRef]
43. Chen, J.; Yang, H.; Wang, N.; Ring, Z.; Dabros, T. Mathematical modeling of monolith catalysts and reactors for gas phase reactions. *Appl. Catal. A Gen.* **2008**, *345*, 1–11. [CrossRef]
44. Hayes, R.E.; Cornejo, I. Multi-scale modelling of monolith reactors: A 30-year perspective from 1990 to 2020. *Can. J. Chem. Eng.* **2021**, *99*, 2589–2606. [CrossRef]
45. Kunst, J.A.F.; Cybulski, A.; Xiaoding, X.; Moulijn, J.A. Estimation of kinetic parameters from non-isothermally operated monolithic reactors: Oxidation of carbon monoxide. *Chem. Eng. Sci.* **1995**, *50*, 2845–2852. [CrossRef]
46. Roy, S.; Bauer, T.; Al-Dahhan, M.; Lehner, P.; Turek, T. Monoliths as multiphase reactors: A review. *AIChE J.* **2004**, *50*, 2918–2938. [CrossRef]
47. Moulijn, J.A.; Kreutzer, M.T.; Nijhuis, T.A.; Kapteijn, F. Monolithic Catalysts and Reactors: High Precision with Low Energy Consumption. *Adv. Catal.* **2011**, *54*, 249–327. [CrossRef]
48. Balakotaiah, V.; Sun, Z.; Ratnakar, R. Ignition–extinction analysis of catalytic reactor models. *Rev. Chem. Eng.* **2021**, *38*, 737–768. [CrossRef]
49. Heck, R.M.; Farrauto, R.J.; Gulati, S.K. *Catalytic Air Pollution Control: Commercial Technology*, 3rd ed.; Wiley: Hoboken, NJ, USA, 2016; pp. 1–544.

50. Chu, S.; Wang, E.; Feng, F.; Zhang, C.; Jiang, J.; Zhang, Q.; Wang, F.; Bing, L.; Wang, G.; Han, D.A. Review of noble metal catalysts for catalytic removal of VOCs. *Nanostruct Catal. Appl. Environ.* **2022**, *12*, 1543. [CrossRef]
51. Wang, S.; Li, X.; Lai, C.; Zhang, Y.; Lin, X.; Ding, S. Recent advances in noble metal-based catalysts for CO oxidation. *RSC Adv.* **2024**, *14*, 30566. [CrossRef] [PubMed]
52. Lin, F.; Hoang, D.T.; Tsung, C.K. Catalytic properties of Pt cluster-decorated CeO_2 nanostructures. *Nano Res.* **2011**, *4*, 61–71. [CrossRef]
53. Kozhukhova, A.E.; Govender, A.; Marx, G.; Olivier, E.J.; Bessarabov, D.G. The effect of reduction temperature and Zn doping on the catalytic activity of Pt–Al_2O_3 catalyst for catalytic H_2/O_2 recombination. *Int. J. Hydrogen Energy* **2026**, *197*, 152604. [CrossRef]
54. Muravev, V.; Simons, J.F.M.; Parastaev, A.; Verheijen, M.A.; Struijs, J.J.C.; Kosinov, N.; Hensen, E.J.M. Operando Spectroscopy Unveils the Catalytic Role of Different Palladium Oxidation States in CO Oxidation on Pd/CeO_2 Catalysts. *Angew. Chem. Int. Ed.* **2022**, *61*, 1–10. [CrossRef]
55. Kaichev, V.V.; Saraev, A.A.; Fedorov, A.V.; Gerasimov, E.Y. The Origin of the Size Effect in the Oxidation of CO on Supported Palladium Nanoparticles. *Catalysts* **2023**, *13*, 1435. [CrossRef]
56. Zongbo, S.; Qing, Z.; Guangpeng, Y.; Liang, L.; Gang, W.; Rizki, E.; Ismal, G.; Ruilin, W.; Runsheng, Z. Au supported on γ-AlOOH and γ-Al_2O_3 for low temperature oxidation of CO and aromatic alcohols. *RSC Adv.* **2025**, *15*, 7563–7570. [CrossRef]
57. Kohno, A.; Ito, S.; Kato, K.; Minowa, H.; Aratake, A.; Maruo, Y.Y. Synthesis, characterization, and photocatalytic properties of Au nanoparticle-anchored TiO_2 and $CaCO_3$ core–shell composite particles. *Thin Solid. Film.* **2025**, *823*, 140706. [CrossRef]
58. Zhang, S.; Feng, X.; Rao, C.; Xu, X.; Xu, J.; Fang, X.; Li, Y.; Wang, X. Engineering low Pd content catalysts for soot combustion through tuning the Pd-SnO_2 interface interaction: Disclosing the critical role of dual Pd valence states for the activity. *Appl. Catal. A Gen.* **2022**, *647*, 118906. [CrossRef]
59. Fu, Y.; Yin, Z.; Qin, L.; Huang, D.; Yi, H.; Liu, X.; Liu, S.; Zhang, M.; Li, B.; Li, L.; et al. Recent progress of noble metals with tailored features in catalytic oxidation for organic pollutants degradation. *J. Hazard. Mater.* **2022**, *422*, 126950. [CrossRef] [PubMed]
60. Petkov, V.; Ren, Y.; Shan, S.; Luo, J.; Zhong, C.J. A distinct atomic structure catalytic activity relationship in 3-10 nm supported Au particle. *RSC Nanoscale* **2014**, *6*, 532–538. [CrossRef]
61. Guo, Y.; Gu, D.; Jin, Z.; Du, P.-P.; Si, R.; Tao, J.; Xu, W.-Q.; Huang, Y.-Y.; Senanayake, S.; Song, Q.-S.; et al. Uniform 2 nm gold nanoparticles supported on iron oxides as active catalysts for CO oxidation reaction: Structure–activity relationship. *RSC Nanoscale* **2015**, *7*, 4920–4928. [CrossRef]
62. Milt, V.G.; Ivanova, S.; Sanz, O.; Domínguez, M.I.; Corrales, A.; Odriozola, J.A.; Centeno, M.A. Au/TiO2 supported on ferritic stainless steel monoliths as CO oxidation catalysts. *Appl. Surf. Sci.* **2013**, *270*, 169–177. [CrossRef]
63. Della Pina, C.; Dimitratos, N.; Falleta, E.; Rossi, M.; Siani, A. Catalytic performance of gold catalysts in the total oxidation of VOCs. *Gold Bull.* **2007**, *40*, 67–72. [CrossRef]
64. Li, Z.; Hong, R.; Zhang, Z.; Wang, H.; Wu, X.; Wu, Z. Single-Atom Catalysts in Environmental Engineering: Progress, Outlook and Challenges. *Molecules* **2023**, *28*, 3865. [CrossRef] [PubMed]
65. Zhang, H.; Wang, Z.; Lin, H.; Liu, Y.; Dai, H.; Deng, J. Catalytic oxidation of volatile organic compounds over supported noble metal and single atom catalysts: A review. *J. Environ. Sci.* **2025**, *155*, 858–888. [CrossRef]
66. Chae, S.; Chen, Y.; Yang, J.; Su, J. The stability of single-atom catalysts in thermocatalysis. *Surf. Sci. Tech.* **2024**, *2*, 18. [CrossRef]
67. Xiao, M.; Zhao, T.; Li, Y.; Zhu, B.; Yu, T.; Liu, W.; Zhao, M.; Cui, B. Co_3O_4-Based catalysts for the low-temperature catalytic oxidation of VOCs. *Chem. Cat. Chem.* **2024**, *16*, e202301524. [CrossRef]
68. Bulavchenko, O.A.; Konovalova, V.P.; Saraev, A.A.; Kremneva, A.M.; Rogov, V.A.; Gerasimov, E.Y.; Afonasenko, T.N. The catalytic performance of CO oxidation over MnOx-ZrO_2 catalysts: The role of synthetic routes. *Catalysts* **2023**, *13*, 57. [CrossRef]
69. Zhao, T.; Li, Y.; Wu, C.; Cao, W.; Gong, J.; Xiao, M.; Song, Z.; Shao, Z.; Zhao, M.; Cui, B. Oxidation mechanism and performance control of manganese-based catalysts in soot oxidation. *Green Energy Environ.* **2025**, *10*, 1481–1502. [CrossRef]
70. Soltan, W.B.; Sun, J.; Wang, W.; Song, Z.; Zhao, X.; Mao, Y.; Zhang, Z. Discovering the key role of MnO_2 and CeO_2 particles in the Fe_2O_3 catalysts for enhancing the catalytic oxidation of VOC: Synergistic effect of the lattice oxygen species and surface-adsorbed oxygen. *Sci. Total Environ.* **2022**, *819*, 152844. [CrossRef] [PubMed]
71. Ye, Z.; Liu, Y.; Nikiforov, A.; Ji, J.; Zhao, B.; Wang, J. The research on CO oxidation over Ce–Mn oxides: The preparation method effects and oxidation mechanism. *Chemosphere* **2023**, *336*, 139130. [CrossRef] [PubMed]
72. Zhang, Z.; Wang, Y.; Li, X. Interfacial synergy of Ce–Mn oxides toward enhanced catalytic oxidation: Role of oxygen vacancies and lattice oxygen mobility. *Appl. Catal. B Environ.* **2023**, *330*, 122630.
73. Liu, X.; Zhou, K.; Wang, L.; Wang, B.; Li, Y. Oxygen Vacancy Clusters Promoting Reducibility and Activity of Ceria Nanorods. *J. Am. Chem. Soc.* **2009**, *131*, 3140–3141. [CrossRef] [PubMed]
74. Li, Y.; Qin, T.; Ma, Y.; Xiong, J.; Zhang, P.; Lai, K.; Liu, X.; Zhao, Z.; Liu, J.; Chen, L.; et al. Revealing active edge sites induced by oriented lattice bending of Co-CeO_2 nanosheets for boosting auto-exhaust soot oxidation. *J. Catal.* **2023**, *421*, 351–364. [CrossRef]
75. Li, Q.; Wang, X.; Xin, Y.; Zhang, Z.; Zhang, Y.; Hao, C.; Meng, M.; Zheng, L.; Zheng, L. Aunified intermediate and mechanism for soot combustion on potassium supported oxides. *Sci. Rep.* **2014**, *4*, 4725. [CrossRef] [PubMed]

76. Yu, J.; Li, H.; Lin, N.; Gong, Y.; Jiang, H.; Chen, J.; Wang, Y.; Zhang, X. Oxygen-Deficient Engineering for Perovskite Oxides in the Application of AOPs: Regulation, Detection, and Reduction Mechanism. *Catalysts* **2023**, *13*, 148. [CrossRef]
77. Wang, Y.; Chen, G.; Xie, J.; Chen, D. Non-metal/metalloid modification of perovskite oxide enables lattice oxygen participation in accelerating oxygen evolution activity. *Inter. J. Hydrogen Energy* **2022**, *47*, 39108–39119. [CrossRef]
78. Lv, L.; Zhang, Z.; Wang, S.; Shan, Y.; Wang, L.; Xu, T.; He, P. Catalytic oxidation of ethyl acetate over Y (Y = Cu, Mn, Co)-modified CeO_2 derived from Ce-MOF. *Catal. Commun.* **2024**, *186*, 106832. [CrossRef]
79. Orfanoudaki, A.; Lykaki, M.; Bonis, A.K.; Saini, S.; Dury, G.; Mutch, G.A.; Papaioannou, E.I.; Kousi, K.; Konsolakis, M. Facet-dependent metal–support interactions in cobalt–ceria binary oxides: Linking ceria morphology (rods vs. cubes) to redox behaviour and CO oxidation. *Catal. Sci. Technol.* **2026**, *16*, 2716–2728. [CrossRef]
80. Chudinovych, O.V.; Tomila, T.V.; Kolesnichenko, V.G.; Samelyuk, A.V.; Vedel, D.V.; Lynnyk, A. Phase relations in the Sm_2O_3-Fe_2O_3 system: Structure and magnetic properties of perovskite $SmFeO_3$ ceramics. *Open Ceram.* **2025**, *24*, 100866. [CrossRef]
81. McCarty, J.G.; Gusman, M.; Lowe, D.M.; Hildenbrand, D.L.; Lau, K.N. Stability of supported metal and supported metal oxide combustion catalysts. *Catal. Today* **1999**, *47*, 5–17. [CrossRef]
82. Védrine, J.C. Metal Oxides in Heterogeneous Oxidation Catalysis: State of the Art and Challenges for a More Sustainable World. *Chem. Sus. Chem.* **2019**, *12*, 577–588. [CrossRef]
83. Gremminger, A.; Lott, P.; Merts, M.; Casapu, M.; Grunwaldt, J.D.; Deutschmann, O. Sulfur poisoning and regeneration of bimetallic Pd–Pt methane oxidation catalysts. *Appl. Catal. B Environ.* **2017**, *218*, 833–843. [CrossRef]
84. Lott, P.; Eck, M.; Doronkin, D.E.; Zimina, A.; Tischer, S.; Popescu, R.; Belin, S.; Briois, V.; Casapu, M.; Grunwaldt, J.-D.; et al. Understanding sulfur poisoning of bi-metallic Pd–Pt methane oxidation catalysts and their regeneration. *Appl. Catal. B Environ.* **2020**, *278*, 119244. [CrossRef]
85. Wang, C.; Hou, X.; Jin, L.; Li, J.; Gu, L.; Yang, L. Review on the impact of SO_2 on VOCs oxidation: Mechanisms and anti-poisoning strategies. *Fuel* **2024**, *359*, 130450. [CrossRef]
86. Pinard, L.; Batiot-Dupeyrat, C. Non-thermal plasma for catalyst regeneration: A review. *Catal. Today* **2024**, *426*, 114372. [CrossRef]
87. Orihuela, M.P.; Miceli, P.; Ramírez-Rico, J.; Fino, D.; Chacartegui, R. Ceria-based catalytic coatings on biomorphic silicon carbide: A system for soot oxidation with enhanced properties. *Chem. Eng. J.* **2021**, *415*, 128959. [CrossRef]
88. Leonardi, S.A.; Miró, E.E.; Milt, V.G. Ceramic Papers as Structured Catalysts: Preparation and Application for Particulate Removal. *Catalysts* **2022**, *12*, 1153. [CrossRef]
89. Reichelt, E.; Heddrich, M.P.; Jahn, M.; Michaelis, A. Fiber based structured materials for catalytic application. *Appl. Catal. A Gen.* **2014**, *476*, 78–90. [CrossRef]
90. Matatov-Meytal, Y.; Sheintuch, M. Catalytic fibers and cloths. *Appl. Catal. A Gen.* **2002**, *231*, 1–16. [CrossRef]
91. Cooke, T.F. Fibers as supports for catalysts: A survey of the literature. *J. Polym. Eng.* **1990**, *9*, 1–22. [CrossRef]
92. Xin, B.; Gao, W.; Ji, Z.; Zhang, S.; Xin, L.; Zhao, L.; Xue, H.; Wu, Q.; Zhang, L.; Liu, C.; et al. Carbon fiber-promoted activation of catalyst for efficient growth of single-walled carbon nanotubes. *Carbon N. Y.* **2020**, *156*, 410–415. [CrossRef]
93. Ptaszyńska, K.; Malaika, A.; Kapska, M.; Kozłowski, M. SO3H-functionalized carbon fibers for the catalytic transformation of glycerol to glycerol tert-butyl ethers. *Sci. Rep.* **2023**, *13*, 565. [CrossRef] [PubMed]
94. Rodriguez, M. Fibrous Catalysts for Environmental Application. Ph.D. Thesis, Universidad Nacional del Litoral, Santa Fe, Argentina, 2025.
95. Stegmayer, M.A.; Milt, V.G.; Miró, E.E. Biomorphic synthesis of cobalt oxide and ceria microfibers. Their application in diesel soot oxidation. *Catal. Commun.* **2020**, *139*, 105984. [CrossRef]
96. Rodriguez, M.; Leonardi, S.A.; Hanon, F.; Miró, E.E.; Milt, V.G.; Gaigneaux, E.M. Plasma-assisted deposition of Mn and Fe phases on CeO_2 biomorphic fibers for soot combustion and CO oxidation. *Catal. Today* **2024**, *431*, 114457. [CrossRef]
97. Rodriguez, M.; Hanon, F.; Devred, F.; Gaigneaux, E.M.; Miró, E.E.; Milt, V.G. Mn and Co decorated biomorphic ceria fiber catalysts for soot and benzene total oxidation. *Chemosphere* **2024**, *359*, 142247. [CrossRef] [PubMed]
98. Sacco, N.A.; Banús, E.D.; Bortolozzi, J.P.; Leonardi, S.A.; Miró, E.E.; Milt, V.G. Synthesis and Catalytic Performance of Cotton-Derived Mn–Ce and Mn–Co–Ce Biomorphic Fibers for Soot Combustion and CO Oxidation. *Sustain. Chem.* **2025**, *6*, 20. [CrossRef]
99. Leonardi, S.A.; Rodriguez, M.; Miró, E.E.; Gaigneaux, E.M.; Milt, V.G. The Use of the Gliding Arc Plasma Technique to Deposit Fe or Mn Oxides on Fibrous Ceramic Supports for Reactions of Environmental Interest. *Materials* **2025**, *18*, 5479. [CrossRef] [PubMed]
100. Stegmayer, M.A. Síntesis, Caracterización Y Evaluación de Catalizadores Basados en Fibras Para Reacciones de Oxidación. Ph.D. Thesis, Universidad Nacional del Litoral, Santa Fe, Argentina, 2021.
101. Wu, H.; Pan, W.; Lin, D.; Li, H. Electrospinning of ceramic nanofibers: Fabrication, assembly and applications. *J. Adv. Ceram.* **2012**, *1*, 2–23. [CrossRef]
102. Stegmayer, M.A.; Irusta, S.; Miró, E.E.; Milt, V.G. Electrospinning synthesis and characterization of nanofibers of Co, Ce and mixed Co-Ce oxides. Their application to oxidation reactions of diesel soot and CO. *Catal. Today* **2022**, *383*, 266–276. [CrossRef]

103. Liao, Y.; Liu, P.; Zhang, J.; Wang, C.; Chen, L.; Yan, D.; Ren, Q.; Liang, X.; Fu, M.; Suib, S.L. Electrospun Ce-Mn oxide as an efficient catalyst for soot combustion: Ce-Mn synergy, soot-catalyst contact, and catalytic oxidation mechanism. *Chemosphere* **2023**, *334*, 138995. [CrossRef] [PubMed]
104. Sim, M.; Wang, B.; Oh, T.-S. Low temperature CO oxidation by doped cerium oxide electrospun fibers. *Nano Converg.* **2020**, *7*, 22. [CrossRef] [PubMed]
105. Ma, Y.; Ma, Y.; Long, G.; Buckley, C.E.; Hu, X.; Dong, D. Electrospun $La_{0.8}Ce_{0.2}Fe_{1-x}Ni_xO_3$ perovskite nanofibrous catalysts for CO oxidation. *Appl. Surf. Sci. Adv.* **2020**, *2*, 100030. [CrossRef]
106. Stegmayer, M.A.; Milt, V.G.; Navascues, N.; Gamez, E.; Irusta, S.; Miró, E.E. Cobalt deposited on micro and nanometric structures of ceria and zirconia applied in diesel soot combustion. *Mol. Catal.* **2020**, *481*, 110636. [CrossRef]
107. Guerrero-Pérez, M.O. Research Progress on the Applications of Electrospun Nanofibers in Catalysis. *Catalysts* **2022**, *12*, 9. [CrossRef]
108. Courtalón, N.L.; Milt, V.G.; Miró, E.E.; Banús, E.D.; Bortolozzi, J.P. Clay-based 3D-printed monoliths impregnated with Co and Ce for the manufacturing of structured catalysts: Their application in soot and CO oxidations. *J. Environ. Chem. Eng.* **2026**, *14*, 121738. [CrossRef]
109. Davó-Quiñonero, A.; Sorolla-Rosario, D.; Bailón-García, E.; Lozano-Castelló, D.; Bueno-López, A. Improved asymmetrical honeycomb monolith catalyst prepared using a 3D printed template. *J. Hazard. Mater.* **2019**, *368*, 638–643. [CrossRef] [PubMed]
110. Yao, J.; Dong, F.; Xu, X.; Wen, M.; Ji, Z.; Feng, H.; Wang, X.; Tang, Z. Rational Design and Construction of Monolithic Ordered Mesoporous Co_3O_4@SiO_2 Catalyst by a Novel 3D Printed Technology for Catalytic Oxidation of Toluene. *ACS Appl. Mater. Interfaces* **2022**, *14*, 22170–22185. [CrossRef] [PubMed]
111. Cepollaro, E.M.; Cimino, S.; D'Agostini, M.; Gargiulo, N.; Franchin, G.; Lisi, L. 3D-Printed Monoliths Based on Cu-Exchanged SSZ-13 as Catalyst for SCR of NOx. *Catalysts* **2024**, *14*, 85. [CrossRef]
112. Song, M.; Kim, Y.; Baek, D.S. 3D microprinting of inorganic porous materials by chemical linking-induced solidification of nanocrystals. *Nat. Commun.* **2023**, *14*, 8460. [CrossRef] [PubMed]
113. Godoy, M.L. Desarrollo de Monolitos Catalíticos de Mallas Metálicas Apiladas Para la Eliminación de Contaminantes Provenientes de Motores Diésel. Ph.D. Thesis, Universidad Nacional del Litoral, Santa Fe, Argentina, 2020.
114. Godoy, M.L.; Milt, V.G.; Miró, E.E.; Banús, E.D. Scaling-up of the catalytic stacked wire mesh filters for the abatement of diesel soot. *Catal. Today* **2022**, *394*, 434–444. [CrossRef]
115. Godoy, M.L.; Banus, E.D.; Bon, M.; Miro, E.E.; Milt, V.G. Synthesis of Co, Ce oxide nanoparticles by an aerosol method and their deposition on different structured substrates for catalytic removal of diesel particulate matter. *Catalysts* **2023**, *13*, 660. [CrossRef]
116. Leonardi, S.A.; Miró, E.E.; Milt, V.G. Activity of Catalytic Ceramic Papers to Remove Soot Particles—A Study of Different Types of Soot. *Catalysts* **2022**, *12*, 855. [CrossRef]
117. Tuler, F.E.; Banús, E.D.; Zanuttini, M.A.; Miró, E.E.; Milt, V.G. Ceramic papers as flexible structures for the development of novel diesel soot combustion catalysts. *Chem. Eng. J.* **2014**, *246*, 287–298. [CrossRef]
118. Sacco, N.; Banús, E.D.; Bortolozzi, J.P.; Milt, V.G.; Miró, E.E. Ultrasound-Assisted Deposition of Co–CeO_2 onto Ceramic Microfibers to Conform Catalytic Papers: Their Application in Engine Exhaust Treatment. *ACS Omega* **2018**, *3*, 18334–18342. [CrossRef] [PubMed]
119. Tuler, F.E.; Gaigneaux, E.M.; Miró, E.E.; Milt, V.G.; Debecker, D.P. Catalytic ceramic papers for diesel soot oxidation: A spray method for enhanced performance. *Catal. Commun.* **2015**, *72*, 116–120. [CrossRef]
120. Sacco, N.A.; Bortolozzi, J.P.; Milt, V.G.; Miró, E.E.; Banús, E.D. Ce-Mn oxides synthesized with citric acid on ceramic papers used as diesel particulate filters. *Catal. Today* **2022**, *383*, 277–286. [CrossRef]